Measurement of cytokine production

After a 48-h incubation with LPS, cytokine production was measured using the BD™ Human inflammation cytometric beads array (CBA) kit (BD Biosciences Pharmingen, San Diego, CA) according to the manufacturer's instructions. Briefly, 50 μl of supernatant was stained with a mixture of human cytokine capture bead suspension and the PE detection reagent. After a 3-h incubation, the samples were washed and then analyzed using the BD CBA software. Human inflammatory cytokine standards provided with the kit were appropriately diluted and used in parallel to the samples for the preparation of the standard curves.

Flow cytometric analysis

After a 48-h incubation with LPS, the cells were harvested, washed with PBS and incubated for 15 min on ice with FITC or PE-labeled anti-HLA-DR, CD40, CD80, CD83 and CD86 mAb, or corresponding control mAbs. Cell debris was eliminated from the analysis by forward and side scatter gating. Cell viability was determined by Annexin V-FITC and PI staining for 10 min on ice. Cells were analyzed on the FACSCalibur flow cytometer using the CELLQuest software (Becton Dickinson).

Allogenic mixed leukocyte reaction (MLR)

Allogenic $CD3^+$ T cells were distributed at 5×10^4 per well into round-bottom 96-well microplates. Cells were incubated for 7 days in the presence of 1.7×10^3 of irradiated DC stimulators (25 Gry) in 200 μl of culture medium. T cell proliferation was measured using a CyQUANT kit (Molecular Probes), as previously described (Jones et al., 2001). Briefly, microplates were centrifuged (500 g, 5 min), and then the supernatant was removed and frozen at −80 °C for at least one night. The proliferation was calculated from the change in total nucleic acid content in each well according to the CyQUANT kit that measures the signal generated by the binding of a fluorescent dye to nucleic acids, a signal that increases in proportion to the number of cells (Khanna et al., 1999). The fluorescence signals were read from a 96-well plate using a fluorometric microplate reader (Fluoroskan Ascent; Labsystems, Helsinki, Finland) with excitation and emission wavelengths of 485 and 538 nm, respectively.

Immunoblotting

To examine if nitric oxide (NO) is involved in the LPS-induced maturation of DC, the expression of an inducible isoform of NO synthase (iNOS) was quantified by immunoblotting. After a 4 or 48-h incubation of DC with or without 100 ng/ml LPS, the cells were washed twice with cold PBS and incubated with 50 μl ice-cold lysis buffer (0.1% SDS, 1% NP-40, 5 mM EDTA, 150 mM NaCl, 50 mM Tris–Cl (pH 8.0), 2 mM DTT, 1 mM sodium orthovanadate, and complete protease inhibitor) for 30 min. The homogenates were centrifuged at 4 °C (20,000 g, 15 min). Fifty μg of cell lysates was electrophoresed on 7.5% SDS-PAGE gels and transferred to polyvinylidene–difluoride membranes (Immunobilon-P; Millipore, Bedford, MA). As a positive control, the lysate obtained from the mouse macrophages stimulated by interferon γ plus LPS was loaded in parallel. After blocking with 5% non-fat dried milk, membranes were incubated with human anti-iNOS antibody (BD Biosciences, San Jose, CA) for 12 h at 4 °C and then incubated with horseradish peroxidase-conjugated mouse monoclonal antibody for mouse IgG (Cell signaling, Beverly, MA) for 1 h. Immunoreactive bands were visualized with ECL detection reagent (Amersham, Zurich, Switzerland).

Statistical analyses

Values are shown as means±SD. Statistical comparisons were made using a one-way ANOVA followed by Student's paired *t*-test with a Bonferroni correction. P values <0.05 were regarded as being statistically significant.

Results

LPS-induced ROS generation in DC and its attenuation by PBN and GSH-OEt

The LPS-induced ROS generation in DC was examined, using EPR spectroscopy with a spin trap. Weak oxygen radical signals were detected in the EPR spectra obtained

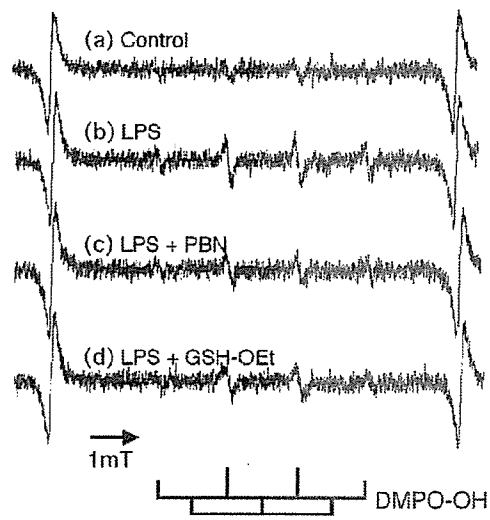

Fig. 1. LPS-induced ROS generation in DC and its attenuation by PBN and GSH-OEt. The EPR spectra obtained from the reaction mixture containing the supernatant of DC incubated with 100 ng ml LPS for 4 h, DETAPAC, DMPO and $FeSO_4$. (a) The DMPO-OH signal is slightly observed in the sample obtained from the DC incubated without LPS. (b) The DMPO-OH signal is clearly observed in that with LPS. The pre-incubation of the DC with (c) 2 mM PBN or (d) 20 mM GSH-OEt for 1 h attenuated the signal intensity of DMPO-OH, which indicated that both PBN and GSH-OEt quenched the generated ROS in the LPS-stimulated DC. Signals appearing both at the high and low field correspond to Mn^{2-} installed in the EPR cavity as a reference. The components of DMPO-OH are indicated by the stick diagram. These data are representative of 5 independent experiments.

from the DC incubated without LPS for 4 h (Fig. 1a). However, in the EPR spectra obtained from the DC incubated with 100 ng/ml LPS for 4 h, stronger oxygen radical signals were observed (Fig. 1b), consisting of a 1:2:2:1 quartet with the hfsc's of a(N)=1.49 mT and a(βH)=1.49 mT, which is indicative of DMPO-OH, a signal of hydroxyl radical (•OH) (Buettner, 1987). In the presence of ferrous ion (Fe^{2+}), •OH is generated via the iron-catalyzed Fenton reaction from hydrogen peroxide (H_2O_2) (Dunford, 1987). In general, H_2O_2 is generated via the superoxide anion ($O_2^{\bullet-}$). Therefore, it is certain that H_2O_2 and/or $O_2^{\bullet-}$ are generated in the LPS-stimulated DC. The pre-incubation of the DC with 2 mM PBN or 20 mM GSH-OEt for 1 h attenuated the signal intensity of DMPO-OH, which indicated that both PBN and GSH-OEt quenched the ROS generated in the LPS-stimulated DC (Fig. 1c and d).

The LPS-induced ROS generation in DC was also confirmed using laser scanning confocal microscopy with the fluorescent dyes, RedoxSensor Red CC-1 and MitoTracker Green FM. Red CC-1 detects total ROS, including $O_2^{\bullet-}$, H_2O_2, and •OH, and MitoTracker is the mitochondrial-selective dye (Shukla et al., 2003; Tanaka et al., 2002). Compared with the control cells, the LPS-stimulated DC showed the ROS accumulation in the mitochondria. The ROS accumulation was attenuated by PBN and GSH-OEt (Fig. 2).

The decline in GSH/GSSG by LPS and its attenuation by GSH-OEt, but not by PBN

When the DC were incubated with 100 ng/ml LPS for 4 h, the GSH/GSSG declined. PBN did not affect the declined

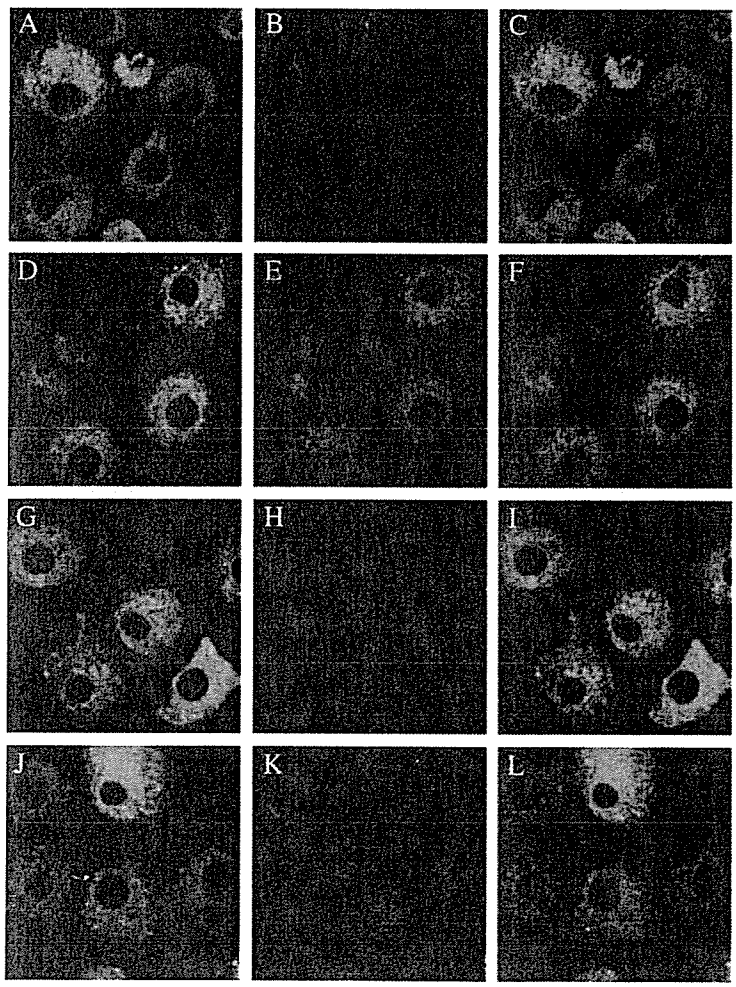

Fig. 2. Intracellular ROS detected by laser scanning confocal microscopy with the oxidant probe, Red CC-1 and the mitochondrial-selective dye, MitoTracker Green. Control cells show little oxidation of Red CC-1 (A–C), while the LPS-stimulated DC show the mitochondrial localization of oxidants (D–F). The LPS-stimulated DC preincubated with 2 mM PBN (G–I) or 20 mM GSH-OEt (J–L) show the reduced fluorescence of Red CC-1. A, D, G and J illustrate mitochondria as detected with MitoTracker Green. B, E, H and K show Red CC-1 localization. C, F, I and L show merged images of MitoTracker Green and Red CC-1. These data are representative of 5 independent experiments. (For interpretation of the references to colour in this figure legend, the reader is referred to the web version of this article.)

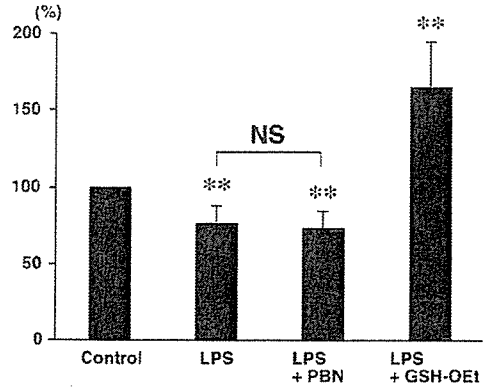

Fig. 3. LPS-induced decline in GSH/GSSG and its attenuation by GSH-OEt not by PBN. The DC were pretreated with 2 mM PBN or 20 mM GSH-OEt for 1 h and then stimulated with 100 ng/ml LPS for 4 h. The cells were harvested and the whole cell extract was prepared. The GSH/GSSG was assessed using the glutathione assay kit as described in the Materials and Methods. The GSH/GSSG in the non-stimulated DC was assigned to 100%. The values are shown as mean ± SD ($n=8$). $^{**}P<0.01$: significantly different from the values obtained from the non-stimulated DC. NS: no significant difference between these two values.

GSH/GSSG, while GSH-OEt counteracted the declined GSH/GSSG in the LPS-stimulated DC (Fig. 3).

Suppression of IL-12p70 and TNF-α production by PBN and GSH-OEt in the LPS-stimulated DC

When the DC were incubated with 100 ng/ml LPS for 48 h, production of TNF-α and IL-12p70 was observed. Pre-incubation with PBN or GSH-OEt suppressed the cytokine production in the LPS-stimulated DC (Fig. 4). Since neither PBN nor GSH-OEt affected the cell viability in the flow cytometric analysis using Annexin V and PI, the possibility of cytotoxic effects of PBN and GSH-OEt was excluded (data not shown).

Suppression of the LPS-induced up-regulation of cell surface molecules by GSH-OEt, but not by PBN

When the DC were incubated with 100 ng/ml LPS for 48 h, the expression of CD40, CD80, CD86, HLA-DR and CD83 was up-regulated. GSH-OEt suppressed the up-regulation of these molecules, while PBN did not affect it in the LPS-stimulated DC (Fig. 5A). The suppression of the up-regulation of surface molecules by GSH-OEt was obscure especially in HLA-DR, probably due to the weak up-regulation of this molecule in the presence of LPS. However, in the molecule with the strong up-regulation such as CD86, GSH-OEt obviously suppressed the up-regulation of this molecule in a dose-dependent manner (Fig. 5B).

Suppression of the allo-stimulatory capacity by GSH-OEt, but not by PBN, in the LPS-stimulated DC

The LPS-stimulated DC exhibited a stronger capacity in inducing T cell proliferation compared with the non-stimulated DC. The enhanced T cell proliferation was suppressed in the DC treated with GSH-OEt, while it was not affected in the DC treated with PBN (Fig. 6).

No induction of the expression of iNOS by LPS in DC

When the DC were incubated with LPS for 4 or 48 h, the expression of iNOS was not observed in immunoblotting (data not shown).

Discussion

In this study, we demonstrated the LPS-induced ROS generation and the concomitant decline in GSH/GSSG in human monocyte-derived DC. Then, we showed that both PBN

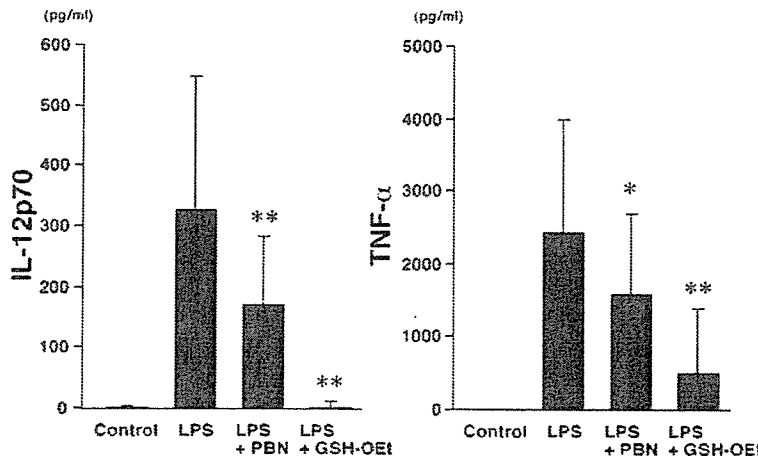

Fig. 4. Suppression of IL-12p70 and TNF-α production by PBN and GSH-OEt in the LPS-stimulated DC. The DC were pretreated with 2 mM PBN or 20 mM GSH-OEt for 1 h and then stimulated with 100 ng/ml LPS for 48 h. The levels of cytokines (TNF-α and IL-12p70) in culture supernatants were measured using the CBA kit as described in Materials and Methods. The values are shown as means ± SD ($n=10$). The mean values of IL-12p70 of the Control, LPS, LPS + PBN and LPS + GSH-OEt were 2, 328, 173 and 4 pg/ml, respectively. Those of TNF-α were 3, 2461, 1617 and 532 pg/ml, respectively. $^{*}P<0.05$ and $^{**}P<0.01$: significantly different from the values obtained from the DC stimulated with LPS alone.

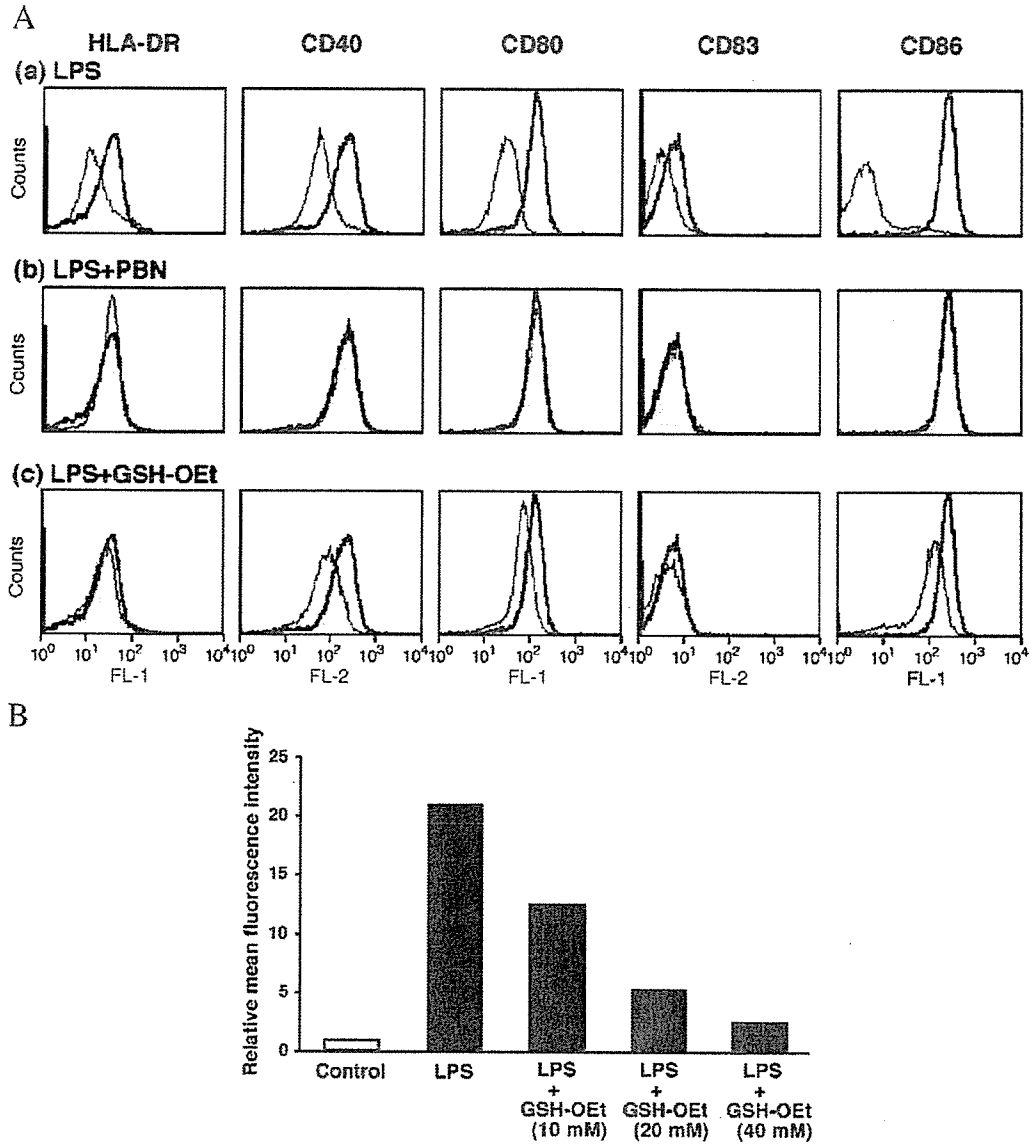

Fig. 5. Suppression of the LPS-induced up-regulation of cell surface molecules by GSH-OEt, but not by PBN. (A) The DC were pretreated with 2 mM PBN or 20 mM GSH-OEt for 1 h and then stimulated with 100 ng/ml LPS for 48 h. The expression of each surface molecule was analyzed with flow cytometry. In the upper panels (a), the open histogram with a fine line shows the expression of each surface molecule in the non-stimulated DC and the open histogram with a bold line shows that in the DC stimulated with LPS alone. In the middle (b) and bottom panels (c), the open histogram with a bold line shows the expression of each surface molecule in the DC stimulated with LPS alone and the filled histogram shows that in the DC pretreated with PBN and GSH-OEt, respectively. These data are representative of 5 independent experiments. (B) The DC were pretreated without or with 10, 20, 40 mM GSH-OEt for 1 h and then stimulated with 100 ng/ml LPS for 48 h. The expression of CD86 was analyzed with flow cytometry. The relative mean fluorescence intensity was calculated when the mean fluorescence intensity obtained from the non-stimulated cells (Control) was assigned to 1, and the mean values obtained from 2 independent experiments are shown.

and GSH-OEt quenched the generated ROS and that only GSH-OEt, and not PBN, counteracted the declined GSH/GSSG. Furthermore, we showed that both PBN and GSH-OEt attenuated the LPS-induced cytokine production and that only GSH-OEt, and not PBN, suppressed the LPS-induced up-regulation of expression of surface molecules and allo-stimulatory capacity in DC.

The LPS-induced ROS generation in DC was demonstrated using EPR spectroscopy. EPR is considered to be the least ambiguous method for the detection of free radicals, because it allows the identification of the original radical (Buettner, 1987). The ROS generation was also confirmed using laser scanning confocal microscopy with Red CC-1. A previous report showed LPS-induced ROS generation in a murine DC line XS52, using flow cytometry with a H_2O_2-sensitive dye, 2′,7′-dichlorofluorescein diacetate (DCFH-DA) (Matsue et al., 2003). However, the fluorescence intensity increased very slightly in LPS-stimulated cells, compared with that in

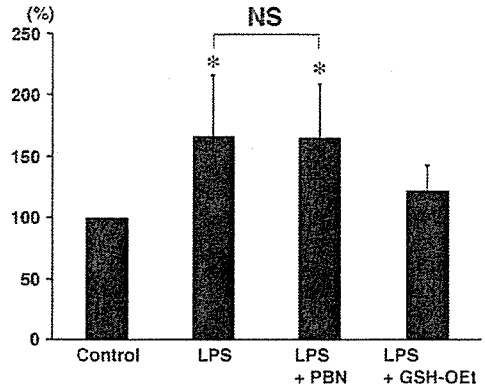

Fig. 6. Suppression of the allo-stimulatory capacity by GSH-OEt, but not by PBN, in the LPS-stimulated DC. The DC were pretreated with 2 mM PBN or 20 mM GSH-OEt for 1 h and then stimulated with 100 ng/ml LPS. After 48 h, the DC were irradiated and cocultured with allogenic T cells at a ratio of 1 DC per 30 T cells for 7 days. T cell proliferation was assessed using the CyQUANT kit as described in the Materials and Methods. The fluorescence signal in T cells cocultured with the non-stimulated DC was assigned to 100%. The values are shown as the means±SD ($n=8$). *$P<0.05$: significantly different from the values obtained from the non-stimulated DC. NS: no significant difference between these two values.

untreated cells. In human monocyte-derived DC, we failed to detect the LPS-induced ROS generation in the flow cytometric analysis with DCFH-DA. DCFH-DA permeates cell membranes, reacts with H_2O_2 and emits green fluorescence by wavelength 488 nm excitation. However, DC themselves have a strong autofluorescence under 488 nm, which may interfere with the weak changes in fluorescence of the dye. On the other hand, Red CC-1 enters live cells, reacts with ROS in the cytosol to yield a red-fluorescent product (excitation/emission maxima ~540/600 nm), which then accumulates in the mitochondria (Chen and Gee, 2000). In the present study, laser scanning confocal microscopy with Red CC-1 showed that DC had no autofluorescence under 543 nm, and that the LPS-stimulated DC had a high level of fluorescence in the mitochondria. Red CC-1 may be more useful than DCFH-DA for the detection of ROS in human DC.

In the present study, LPS brought about the decline in GSH/GSSG. The decline in GSH/GSSG after LPS challenge has been demonstrated in different models of septic shock (Victor et al., 2004). In a mouse septic shock model, a decrease in GSH and an increase in GSSG were observed in peritoneal macrophages and lymphocytes (Victor and De la Fuente, 2003). In children with sepsis, blood GSH redox ratios (GSSG:GSH) were found to be increased (Nemeth and Boda, 2001). These reports all indicate that the decline in GSH/GSSG also occurs in the LPS-stimulated DC.

PBN quenched the generated ROS but did not affect the declined GSH/GSSG in the LPS-stimulated DC. PBN suppressed the cytokine production but did not affect the up-regulation of surface molecules and the allo-stimulatory capacity. GSH-OEt quenched the generated ROS and counteracted the declined GSH/GSSG in the LPS-stimulated DC. GSH-OEt suppressed the cytokine production, the up-regulation of surface molecules and the allo-stimulatory capacity. The capacity of T cell proliferation by DC correlated with expression of costimulatory and MHC molecules and it was not dependent on IL-12 production in DC (Tourkova et al., 2001; Verhasselt et al., 1997). Therefore, our findings suggest that ROS generation is involved in cytokine production, while the declined GSH/GSSG is involved in the up-regulation of cell surface molecules and allo-stimulatory capacity in the LPS-stimulated DC.

NO may also modulate DC function. However, in human monocyte-derived DC, neither release of NO nor iNOS induction after LPS treatment was shown in other studies (Paolucci et al., 2000; Rutault et al., 1999). Also in the present study, the iNOS induction was not observed. Therefore, NO is not likely to be involved in the maturation of human monocyte-derived DC.

LPS induces the activation of an intracellular signaling cascade via Toll-like receptor 4 (Poltorak et al., 1998). The signaling cascade consists of two distinct pathways, the MyD88-dependent and independent pathways (Adachi et al., 1998; Kawai et al., 1999; Takeuchi et al., 2000). It was reported that the MyD88-dependent pathway is involved in cytokine production, while the MyD88-independent pathway is involved in the up-regulation of CD80 and CD86 in DC (Akira et al., 2001; Kaisho et al., 2001). Therefore, our findings may indicate that ROS generation is involved in the MyD88-dependent pathway, while the declined GSH/GSSG is involved in the MyD88-independent pathway. An examination concerning intracellular signal transduction will be required to verify this hypothesis.

In conclusion, the LPS-induced ROS generation and the concomitant decline in GSH/GSSG were observed in the human monocyte-derived DC. They are likely to relate to the maturation of DC in different ways. In fact, suppression of the cytokine production and that of the allo-stimulatory capacity were dissociated and associated by using PBN and GSH-OEt, respectively. The survival or death in sepsis and graft-versus-host disease depends on the balance between inflammatory and immune responses, and it was reported that PBN ameliorates LPS-induced septic shock in rats (Sang et al., 1999) and that GSH depletion contributes to organ injury after bone marrow transplantation (Ziegler et al., 2001). Therefore, the differential regulation of ROS generation and the declined GSH/GSSG may be useful as therapeutic tools in diseases in which inflammatory and immune responses become entangled, such as sepsis and graft-versus-host disease.

References

Adachi, O., Kawai, T., Takeda, K., Matsumoto, M., Tsutsui, H., Sakagami, M., Nakanishi, K., Akira, S., 1998. Targeted disruption of the MyD88 gene results in loss of IL-1- and IL-18-mediated function. Immunity 9 (1), 143–150.

Akira, S., Takeda, K., Kaisho, T., 2001. Toll-like receptors: critical proteins linking innate and acquired immunity. Nature Immunology 2 (8), 675–680.

Anderson, M.E., Powrie, F., Puri, R.N., Meister, A., 1985. Glutathione monoethyl ester: preparation, uptake by tissues, and conversion to glutathione. Archives of Biochemistry and Biophysics 239 (2), 538–548.

Banchereau, J., Steinman, R.M., 1998. Dendritic cells and the control of immunity. Nature 392 (6673), 245–252.

Buettner, G.R., 1987. Spin trapping: ESR parameters of spin adducts. Free Radical Biology and Medicine 3 (4), 259–303.

Cella, M., Engering, A., Pinet, V., Pieters, J., Lanzavecchia, A., 1997. Inflammatory stimuli induce accumulation of MHC class II complexes on dendritic cells. Nature 388 (6644), 782–787.

Chen, C.S., Gee, K.R., 2000. Redox-dependent trafficking of 2,3,4,5, 6-pentafluorodihydrotetramethylrosamine, a novel fluorogenic indicator of cellular oxidative activity. Free Radical Biology and Medicine 28 (8), 1266–1278.

Dunford, H.B., 1987. Free radicals in iron-containing systems. Free Radical Biology and Medicine 3 (6), 405–421.

Griffith, O.W., 1980. Determination of glutathione and glutathione disulfide using glutathione reductase and 2-vinylpyridine. Analytical Biochemistry 106 (1), 207–212.

Ho, E., Chen, G., Bray, T.M., 2000. Alpha-phenyl-*tert*-butylnitrone (PBN) inhibits NFκB activation offering protection against chemically induced diabetes. Free Radical Biology and Medicine 28 (4), 604–614.

Jones, L.J., Gray, M., Yue, S.T., Haugland, R.P., Singer, V.L., 2001. Sensitive determination of cell number using the CyQUANT cell proliferation assay. Journal of Immunological Methods 254 (1–2), 85–98.

Kaisho, T., Takeuchi, O., Kawai, T., Hoshino, K., Akira, S., 2001. Endotoxin-induced maturation of MyD88-deficient dendritic cells. Journal of Immunology 166 (9), 5688–5694.

Kawai, T., Adachi, O., Ogawa, T., Takeda, K., Akira, S., 1999. Unresponsiveness of MyD88-deficient mice to endotoxin. Immunity 11 (1), 115–122.

Khanna, R., Chang, M.C., Joiner, W.J., Kaczmarek, L.K., Schlichter, L.C., 1999. hSK4/hIK1, a calmodulin-binding KCa channel in human T lymphocytes. Roles in proliferation and volume regulation. Journal of Biological Chemistry 274 (21), 14838–14849.

Kuppner, M.C., Scharner, A., Milani, V., Von Hesler, C., Tschop, K.E., Heinz, O., Issels, R.D., 2003. Ifosfamide impairs the allostimulatory capacity of human dendritic cells by intracellular glutathione depletion. Blood 102 (10), 3668–3674.

Matsue, H., Edelbaum, D., Shalhevet, D., Mizumoto, N., Yang, C., Mummert, M.E., Ocda, J., Masayasu, H., Takashima, A., 2003. Generation and function of reactive oxygen species in dendritic cells during antigen presentation. Journal of Immunology 171 (6), 3010–3018.

Murata, Y., Ohteki, T., Koyasu, S., Hamuro, J., 2002. IFN-gamma and pro-inflammatory cytokine production by antigen-presenting cells is dictated by intracellular thiol redox status regulated by oxygen tension. European Journal of Immunology 32 (10), 2866–2873.

Nemeth, I., Boda, D., 2001. Xanthine oxidase activity and blood glutathione redox ratio in infants and children with septic shock syndrome. Intensive Care Medicine 27 (1), 216–221.

Paolucci, C., Rovere, P., De Nadai, C., Manfredi, A.A., Clementi, E., 2000. Nitric oxide inhibits the tumor necrosis factor α-regulated endocytosis of human dendritic cells in a cyclic GMP-dependent way. Journal of Biological Chemistry 275 (26), 19638–19644.

Poltorak, A., He, X., Smirnova, I., Liu, M.Y., Van Huffel, C., Du, X., Birdwell, D., Alejos, E., Silva, M., Galanos, C., Freudenberg, M., Ricciardi-Castagnoli, P., Layton, B., Beutler, B., 1998. Defective LPS signaling in C3H/HeJ and C57BL/10ScCr mice: mutations in Tlr4 gene. Science 282 (5396), 2085–2088.

Rutault, K., Alderman, C., Chain, B.M., Katz, D.R., 1999. Reactive oxygen species activate human peripheral blood dendritic cells. Free Radical Biology and Medicine 26 (1–2), 232–238.

Sallusto, F., Lanzavecchia, A., 1994. Efficient presentation of soluble antigen by cultured human dendritic cells is maintained by granulocyte/macrophage colony-stimulating factor plus interleukin 4 and downregulated by tumor necrosis factor α. Journal of Experimental Medicine 179 (4), 1109–1118.

Sang, H., Wallis, G.L., Stewart, C.A., Kotake, Y., 1999. Expression of cytokines and activation of transcription factors in lipopolysaccharide-administered rats and their inhibition by phenyl *N*-*tert*-butylnitrone (PBN). Archives of Biochemistry and Biophysics 363 (2), 341–348.

Shukla, A., Jung, M., Stern, M., Fukagawa, N.K., Taatjes, D.J., Sawyer, D., Van Houten, B., Mossman, B.T., 2003. Asbestos induces mitochondrial DNA damage and dysfunction linked to the development of apoptosis. American Journal of Physiology. Lung Cellular and Molecular Physiology 285 (5), L1018–L1025.

Takahashi, A., Yamamoto, K., Okuma, M., Sasada, M., 1992. Transient calcium elevation in polymorphonuclear leukocytes triggered by thrombin-activated platelets. European Journal of Haematology 48 (4), 196–201.

Takeuchi, O., Kaufmann, A., Grote, K., Kawai, T., Hoshino, K., Morr, M., Muhlradt, P.F., Akira, S., 2000. Cutting edge: preferentially the R-stereoisomer of the mycoplasmal lipopeptide macrophage-activating lipopeptide-2 activates immune cells through a toll-like receptor 2- and MyD88-dependent signaling pathway. Journal of Immunology 164 (2), 554–557.

Tanaka, H., Matsumura, I., Ezoe, S., Satoh, Y., Sakamaki, T., Albanese, C., Machii, T., Pestell, R.G., Kanakura, Y., 2002. E2F1 and c-Myc potentiate apoptosis through inhibition of NF-κB activity that facilitates MnSOD-mediated ROS elimination. Molecular Cell 9 (5), 1017–1029.

Tourkova, I.L., Yurkovetsky, Z.R., Shurin, M.R., Shurin, G.V., 2001. Mechanisms of dendritic cell-induced T cell proliferation in the primary MLR assay. Immunology Letters 78 (2), 75–82.

Verhasselt, V., Buelens, C., Willems, F., De Groote, D., Haeffner-Cavaillon, N., Goldman, M., 1997. Bacterial lipopolysaccharide stimulates the production of cytokines and the expression of costimulatory molecules by human peripheral blood dendritic cells: evidence for a soluble CD14-dependent pathway. Journal of Immunology 158 (6), 2919–2925.

Verhasselt, V., Vanden Berghe, W., Vanderheyde, N., Willems, F., Haegeman, G., Goldman, M., 1999. *N*-acetyl-L-cysteine inhibits primary human T cell responses at the dendritic cell level: association with NF-κB inhibition. Journal of Immunology 162 (5), 2569–2574.

Victor, V.M., De la Fuente, M., 2003. Immune cells redox state from mice with endotoxin-induced oxidative stress. Involvement of NF-kappaB. Free Radical Research 37 (1), 19–27.

Victor, V.M., Rocha, M., De la Fuente, M., 2004. Immune cells: free radicals and antioxidants in sepsis. International Immunopharmacology 4 (3), 327–347.

Zhou, L.J., Tedder, T.F., 1996. CD14^{+} blood monocytes can differentiate into functionally mature CD83^{+} dendritic cells. Proceedings of the National Academy of Sciences of the United States of America 93 (6), 2588–2592.

Ziegler, T.R., Panoskaltsus-Mortari, A., Gu, L.H., Jonas, C.R., Farrell, C.L., Lacey, D.L., Jones, D.P., Blazar, B.R., 2001. Regulation of glutathione redox status in lung and liver by conditioning regimens and keratinocyte growth factor in murine allogeneic bone marrow transplantation. Transplantation 72 (8), 1354–1362.

Virus-stimulated plasmacytoid dendritic cells induce CD4$^+$ cytotoxic regulatory T cells

Kazuko Kawamura, Norimitsu Kadowaki, Toshio Kitawaki, and Takashi Uchiyama

Immune responses to pathogens need to be maintained within appropriate levels to minimize tissue damage, whereas such controlled immunity may allow persistent infection of certain types of pathogens. Interleukin 10 (IL-10) plays an important role in such immune regulation. We previously showed that HSV-stimulated human plasmacytoid dendritic cells (pDCs) induced naive CD4$^+$ T cells to differentiate into interferon γ (IFN-γ)/IL-10–producing T cells. Here we show that HSV-stimulated pDCs induce allogeneic naive CD4$^+$ T cells to differentiate into cytotoxic regulatory T cells that poorly proliferate on restimulation and inhibit proliferation of coexisting naive CD4$^+$ T cells. IL-3–stimulated pDCs or myeloid DCs did not induce such regulatory T cells. Both IFN-α and IL-10 were responsible for the induction of anergic and regulatory properties. High percentages of CD4$^+$ T cells cocultured with HSV-stimulated pDCs, and to a lesser extent those cocultured with IL-3–stimulated pDCs, expressed granzyme B and perforin in an IL-10–dependent manner. CD4$^+$ T cells cocultured with HSV-stimulated pDCs accordingly exhibited cytotoxic activity. The finding that virus-stimulated pDCs are capable of inducing CD4$^+$ cytotoxic regulatory T cells suggests that this DC subset may play an important role in suppressing excessive inflammatory responses and also in inducing persistent viral infection. (Blood. 2006;107:1031-1038)

Introduction

Maintaining the strength of immune responses to pathogens within appropriate levels is important in eliminating the pathogens without accompanying pathologic inflammatory responses. Such well-balanced immunity can be achieved by simultaneous secretion of an anti-inflammatory cytokine interleukin 10 (IL-10) together with proinflammatory cytokines. For example, without IL-10, mice infected with *Toxoplasma gondii* succumb to a lethal immune response.[1] On the other hand, IL-10 has been shown to prevent complete eradication of *Leishmania major* after acute infection and to allow persistence after clinical cure.[2,3] Thus, a subtle balance between hosts and pathogens is maintained by IL-10 during immunity to infections.

CD4$^+$ T cells concurrently producing interferon γ (IFN-γ) and IL-10 have been repeatedly isolated from hosts suffering from chronic infections with different types of pathogens such as *Mycobacterium tuberculosis*,[4] *Borrelia*,[5] *Leishmania*,[2] and hepatitis C virus,[6] suggesting the physiologic importance of IFN-γ/IL-10–producing CD4$^+$ T cells. These pathogens are characterized by the tendency to persist after clinical cure, which leaves a risk of reactivation of pathogens in an immunocompromised host. The IL-10 derived from CD4$^+$ T cells may be involved in establishing persistence of pathogens.[2,3,7] An important question is how the IFN-γ/IL-10–producing CD4$^+$ T cells are induced during infections.

Differentiation of naive CD4$^+$ T cells to effector T cells that produce particular sets of cytokines is critically influenced by the type of dendritic cells (DCs). It has been shown that either different subsets of DCs or DCs activated by different stimuli are capable of inducing divergent CD4$^+$ T-cell responses,[8] prototypes of which are Th1 and Th2 responses. In humans, 2 distinct types of DCs exist: myeloid DCs (mDCs) and plasmacytoid DCs (pDCs).[9] Notably, pDCs are well equipped to protect a host from viral infection in that (1) they characteristically express Toll-like receptor 7 (TLR7) and TLR9, which recognize single-stranded RNA and unmethylated CpG DNA derived from viruses, respectively[10]; (2) at the DC precursor stage, pDCs produce vast amounts of type I IFNs (IFN-α/β), essential cytokines in antiviral immunity,[11] in response to viruses[10,12]; and (3) pDCs are able to present viral antigens after infected with viruses.[13,14] Thus, pDCs appear to play a key role in developing and modulating antiviral immune responses.

We previously showed that after producing large amounts of type I IFNs in response to HSV, pDC precursors survive and increase the expression of major histocompatibility complex (MHC) and costimulatory molecules, thus developing to DCs that prime naive CD4$^+$ T cells to differentiate into IFN-γ/IL-10–producing T cells, in contrast to IL-3–stimulated pDCs, which preferentially induce Th2 type cells.[15] This finding implies that virus-stimulated, type I IFN-producing pDCs may be responsible for the induction of the immunoregulatory IFN-γ/IL-10–producing CD4$^+$ T cells during infection with viruses that persist after clinical cure.

Although type I IFNs play a crucial role in eliminating viruses through direct antiviral effects and indirect immune-enhancing effects on various cell types in the immune system,[16] findings are

From the Department of Hematology and Oncology, Graduate School of Medicine, Kyoto University, Kyoto, Japan.

Submitted April 28, 2005; accepted September 25, 2005. Prepublished online as *Blood* First Edition Paper, October 11, 2005; DOI 10.1182/blood-2005-04-1737.

Supported by a research grant from Takeda Science Foundation, Japan. K.K. preformed research and wrote the paper; N.K. designed research and wrote the paper; T.K. contributed vital experimental designs and techniques; and T.U. supervised the whole project.

Reprints: Norimitsu Kadowaki, Department of Hematology and Oncology, Graduate School of Medicine, Kyoto University, 54 Shogoin Kawara-cho, Sakyo-ku, Kyoto 606-8507, Japan; e-mail: kadowaki@kuhp.kyoto-u.ac.jp.

The publication costs of this article were defrayed in part by page charge payment. Therefore, and solely to indicate this fact, this article is hereby marked "advertisement" in accordance with 18 U.S.C. section 1734.

emerging that type I IFNs can also negatively regulate immune responses. For example, failure to induce protective Th1-type immunity to a virulent isolate of *M tuberculosis* is associated with increased induction of type I IFNs.[17] IFN-α together with IL-10 induces differentiation of IL-10– and IFN-γ–producing human type 1 T regulatory (Tr1) cells in vitro.[18] Type I IFNs attenuate the generation of antigen-specific $CD8^+$ T cells apparently through the induction of $CD4^+$ Tr1 cells.[19] Thus, type I IFNs produced by virus-stimulated pDCs may have a role in negatively modulating antiviral immune responses.

Several studies have indicated that perforin and granzymes play an immuoregulatory role. During viral infection, perforin not only performs a cytotoxic function to kill virus-infected cells but also down-regulates excessive antiviral immune responses.[20] Furthermore, recent studies have shown that a particular treatment of naive $CD4^+$ T cells, that is, anti-CD3 plus anti-CD46 stimulation, induces perforin/granzyme B-expressing regulatory T cells that kill autologous immune cells.[21,22] However, antigen-presenting cells (APCs) responsible for the induction of perforin and granzymes in $CD4^+$ T cells remain to be determined.

Here, we investigated whether type I IFN-producing, HSV-stimulated pDCs are capable of inducing $CD4^+$ immunoregulatory T cells. We compared HSV-stimulated pDCs (HSV-pDCs) with IL-3–stimulated pDCs (IL-3–pDCs) and granulocyte-macrophage colony-stimulating factor (GM-CSF)–stimulated mDCs (GM-CSF–mDCs) to examine whether viral stimulation specifically endows pDCs with functions down-regulatory for $CD4^+$ T cells. We show that HSV-pDCs, but not the other 2 types of DCs, induce anergic and regulatory $CD4^+$ T cells in a type I IFN- and IL-10–dependent manner. HSV-pDCs, and to a lesser extent IL-3-pDCs, induce $CD4^+$ T cells that express perforin and granzymes and have cytotoxic activity. These data suggest a novel aspect of immunoregulatory roles of type I IFN-producing pDCs in antiviral immunity.

Materials and methods

Isolation of DCs and T cells

Peripheral blood mononuclear cells (PBMCs) were obtained from buffy coat of healthy donors (kindly provided by Kyoto Red Cross Blood Center, Kyoto, Japan). $CD4^+CD11c^-lin^-$ cells and $CD4^+CD11c^+lin^-$ cells were isolated as pDC precursors and mDCs, respectively, as described,[15] using a FACSAria cell sorter (BD Biosciences, San Jose, CA). Reanalysis of the sorted cells confirmed a purity of more than 98%. Naive $CD4^+$ T cells were isolated by negative selection using the $CD4^+$ T cell isolation kit II (Miltenyi Biotec, Bergisch Gladbach, Germany) from umbilical cord blood obtained with written informed consent.

DC/T-cell coculture

mDCs and pDC precursors were plated in round-bottomed 96-well plates at an initial density of 1×10^5 cells/mL in 100 μL RPMI 1640 (Sigma, St Louis, MO) supplemented with 10% fetal calf serum (FCS; ThermoTrace, Melbourne, Australia), 2 mM L-glutamine, penicillin G, streptomycin (Gibco BRL, Carlsbad, CA), and 10 mM HEPES (nacalai tesque, Kyoto, Japan; referred to as complete medium). Then, 50 ng/mL GM-CSF (a gift from DNAX Research Institute, Palo Alto, CA), 10^6 plaque-forming unit (PFU)/mL HSV-1 (KOS strain, attenuated with UV irradiation, a gift from Dr M. Yasukawa, Ehime University, Ehime, Japan, and Dr Tetsushi Yoshikawa, Fujta Health University, Aichi, Japan), 10 ng/mL IL-3 (PeproTech, London, United Kingdom), or 6 μg/mL oligodeoxynucleotide (ODN) 2216 (Hokkaido System Science, Sapporo, Japan), which has been shown to potently induce pDC precursors to produce IFN-α,[23] was added. After 3 days, 5×10^4 naive $CD4^+$ T cells were added in a final volume of 200 μL/well. T cells were cultured in the presence of 10 U/mL recombinant human IL-2 (a gift from Shionogi Osaka, Japan) and 10 ng/mL IL-15 (PeproTech), which have been shown to enhance proliferation of regulatory T cells without affecting their regulatory function.[24] At day 8, cells were harvested and analyzed for their profile of cytokine production and proliferative capacity. In some experiments, 10 μg/mL mouse anti–human IFN-α/β receptor monoclonal antibody (mAb; PBL Biomedical Laboratories, Piscataway, NJ) or 10 μg/mL anti–human IL-10 mAb (eBioscience, San Diego, CA) was added at day 0 and day 4.

Analysis of intracellular cytokine, granzymes, and perforin by flow cytometry

Intracellular cytokine analysis was performed after 8 days of priming of T cells, as described.[25] Fixed and permeabilized T cells were incubated with phycoerythrin (PE)–conjugated anti-IL-2 or anti-IL-10, and fluorescein isothiocyanate (FITC)–conjugated anti-IFN-γ mAbs. All the mAbs were purchased from BD PharMingen (San Diego, CA). For analysis of granzymes and perforin, T cells stimulated with DCs were stained with anti-CD25-PE (Immunotech, Marseille, France) before fixation, permeabilization, and incubation with FITC-conjugated anti–granzyme A (clone CB9), anti–granzyme B (clone GB11), or anti–perforin mAb (clone δG9). All the mAbs were purchased from BD PharMingen. Cells were analyzed using a FACSCalibur flow cytometer (BD Biosciences), and data were analyzed with CellQuest software (BD Biosciences). For the analysis of granzyme- and perforin-expressing cells, $CD25^+$ cells were gated.

Proliferation of stimulated T cells

T cells stimulated with DCs were tested for their proliferative capacity following second allogeneic activation. Stimulated T cells (5×10^4 cells/well) were restimulated in triplicate with irradiated (4000 rad) allogeneic CD3-depleted PBMCs (1×10^5 cells/well) in a final volume of 200 μL complete medium in 96-well round-bottomed plates. After 4 days of culture, wells were pulsed for 16 hours with 1 μCi/well (0.037 MBq) [^{3}H] thymidine (Amersham, Uppsala, Sweden). Cells were harvested and analyzed in a scintillation counter (TopCount, Packard Instrument, Meriden, CT).

Suppression of naive T-cell proliferation

T cells stimulated with DCs were tested for their ability to suppress the proliferation of naive T cells to allogeneic APCs. Naive $CD4^+$ T cells from cord blood (5×10^4 cells/well) were cocultured in triplicate with irradiated, allogeneic CD3-depleted PBMCs (1×10^5 cells/well), in the absence or presence of stimulated T cells (5×10^4 cells/well) in a final volume of 200 μL in complete medium. Control cultures consisted of naive and stimulated T cells in the absence of allogeneic CD3-depleted PBMCs, and stimulated T cells plus allogeneic CD3-depleted PBMCs in the absence of naive T cells. After 4 days, wells were pulsed for 16 hours with 1 μCi/well (0.037 MBq) [^{3}H] thymidine. Cells were harvested and analyzed in a scintillation counter.

Flow cytometric cytotoxicity assay

Flow cytometric cytotoxicity assay was performed to measure in vitro cellular cytotoxicity of $CD4^+$ T cells in a manner previously described.[22] $CD4^+$ T cells stimulated with DCs were used as effector cells, and human cell lines (Daudi and U937) or activated T cells, which have been shown to be more susceptible to killing than resting T cells,[21] were used as target cells. To prepare activated T cells, total T cells were isolated from PBMCs using CD3 MicroBeads (Miltenyi Biotec), and were stimulated with Dynabeads CD3/CD28 T-cell expander (Dynal, Oslo, Norway) and 50 U/mL IL-2 for 5 days according to the manufacturer's instructions. Daudi and U937 were labeled with 200 nM 5- (and 6-) CFSE (Molecular Probes, Eugene, OR) in PBS for 15 minutes at 37°C in a volume of 1 mL. The activated T cells were stained with CFSE and propidium iodide, and propidium iodide-negative viable cells were isolated using a FACSAria cell sorter. CFSE-labeled target cells were then washed twice in PBS and seeded to round-bottomed 96-well plates. A constant number (2.5×10^4 cells/well)

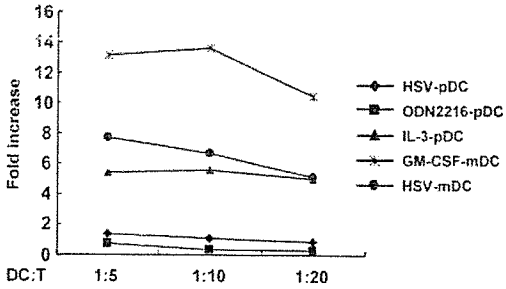

Figure 1. HSV-pDCs induce poor proliferation of naive CD4+ T cells. Allogeneic naive CD4+ T cells (5×10^4) were stimulated with 1×10^4, 5×10^3, or 2.5×10^3 of 5 different types of DCs, as indicated, in 200 μL for 8 days. Fold increases in T-cell numbers during culture are shown. The data shown are representative of more than 10 experiments. ♦ indicates HSV-pDC; ■, ODN2216-pDC; ▲, IL-3-pDC; *, GM-CSF-mDC; ●, HSV-mDC.

of target cells were added along with effector cells at the indicated effector-to-target (E/T) ratios. Cell mixtures were incubated in a total volume of 100 μL complete medium for 4 hours at 37°C. In parallel, target cells were incubated alone to measure basal apoptosis. Immediately before analysis, 1 μg/mL 7-aminoactinomycin D (7-AAD; BD PharMingen) was added to each sample. To analyze the role of the perforin/granzyme pathway in killing, 4 mM EGTA (nacalai tesque) was added to inhibit calcium-dependent perforin polymerization. Samples were analyzed using a FACSCalibur flow cytometer. The percentage of specific lysis was calculated as follows: 100 × (% sample lysis − % basal lysis)/100 − % basal lysis.[26]

Statistical analysis

Data are presented as means plus or minus SD. Statistical comparisons were performed using unpaired 2-tailed Student *t* tests, with a *P* value below .05 taken to indicate significance.

Ethical principles

This study was approved by the institutional review board at the Graduate School of Medicine, Kyoto University, and abides by the tenets of the Declaration of Helsinki.

Results

Virus-stimulated pDCs induce poor proliferation of allogeneic naive CD4+ T cells

First we compared proliferation of allogeneic naive CD4+ T cells stimulated with 5 different types of DCs, specifically, HSV-pDCs, ODN2216-pDCs, IL-3–pDCs, GM-CSF–mDCs, and HSV-mDCs, during primary culture. We stimulated pDCs with HSV, ODN2216, or IL-3 for 3 days, and mDCs with GM-CSF or HSV for 3 days. Allogeneic naive CD4+ T cells were cocultured with these activated pDCs or mDCs at 3 different ratios for 8 days in the presence of 10 U/mL IL-2 and 10 ng/mL IL-15. During the primary culture, T cells stimulated with GM-CSF–mDCs vigorously proliferated, whereas those stimulated with HSV-pDCs or ODN2216-pDCs underwent markedly suppressed proliferation (Figure 1). Proliferation of T cells stimulated with IL-3–pDCs or HSV-mDCs was also poor, although the degree of suppression was less than that observed in T cells stimulated with HSV-pDCs or ODN2216-pDCs. Similar data were obtained at all 3 ratios between DCs and T cells. The poorer proliferation of T cells stimulated with HSV-mDCs than those stimulated with GM-SCF–mDCs is probably due to the absence of TLR9 in mDCs[10] and the resultant absence of activation with HSV.[27] Thus, IFN-α–producing HSV-pDCs and ODN2216-pDCs have a poor capacity to induce naive CD4+ T-cell proliferation. Because stimulation with viruses rather than ODNs is more physiologic, we used HSV-pDCs as IFN-α–producing pDCs in the following experiments.

Allogeneic naive CD4+ T cells cocultured with virus-stimulated pDCs produce both IFN-γ and IL-10 and less IL-2

We have previously shown that HSV-pDCs induce allogeneic naive CD4+ T cells to differentiate into IFN-γ– and IL-10–producing cells.[15] This cytokine profile is similar to that of Tr1 cells,[28] and thus we examined whether these T cells produce a smaller amount of IL-2 than CD4+ T cells that were stimulated with other types of DCs, which is another feature of regulatory T cells.[28] As shown in Figure 2, HSV-pDCs induced a significant number of naive CD4+ T cells to differentiate into IFN-γ/IL-10 double-producing cells, but induced a lower number of IL-2–producing cells than GM-CSF–mDCs. IL-3-pDCs also induced a lower number of IL-2–producing cells than GM-CSF–mDCs, whereas IL-3–pDCs induced a lower number of IFN-γ/IL-10–producing cells than HSV-pDCs. GM-CSF–mDCs induced large numbers of IFN-γ– and IL-2–producing T cells, but not IL-10–producing T cells. These data indicate that HSV-pDCs induce IFN-γ+IL-10+IL-2lo CD4+ T cells that have a cytokine profile similar to Tr1 cells.

HSV-pDCs induce anergic and regulatory CD4+ T cells

A cardinal feature of regulatory T cells is a poor proliferative capacity, that is, anergy, in response to secondary stimulation. Thus, we examined proliferative activity of T cells stimulated with different DCs on restimulation. We cocultured naive CD4+ T cells with allogeneic HSV-pDCs, IL-3–pDCs, or GM-CSF–mDCs for 8 days. Thereafter, we restimulated the CD4+ T cells with T cell–depleted and irradiated PBMCs from the same donor as that of DCs for 5 days and measured [3H] thymidine incorporation during the last 16 hours. As shown in Figure 3A, CD4+ T cells

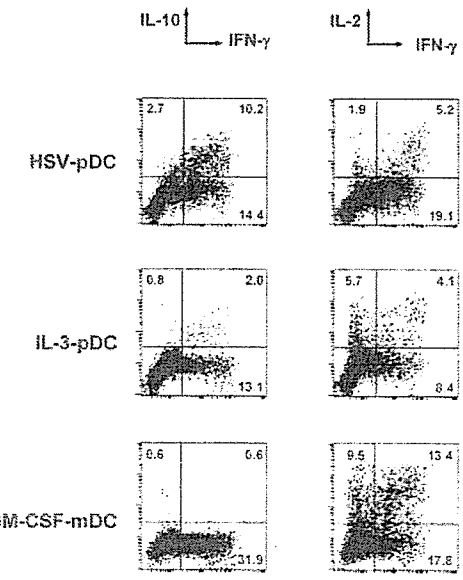

Figure 2. Cytokine production by CD4+ T cells stimulated with HSV-pDCs, IL-3-pDCs, or GM-CSF–mDCs. Naive CD4+ T cells stimulated with allogeneic DCs for 8 days were restimulated with immobilized anti-CD3 and soluble anti-CD28 mAbs in the presence of brefeldin A. After fixation and permeabilization, intracellular cytokine staining was performed. The percentages in each quadrant are indicated on the plot. The data shown are representative of 4 experiments.

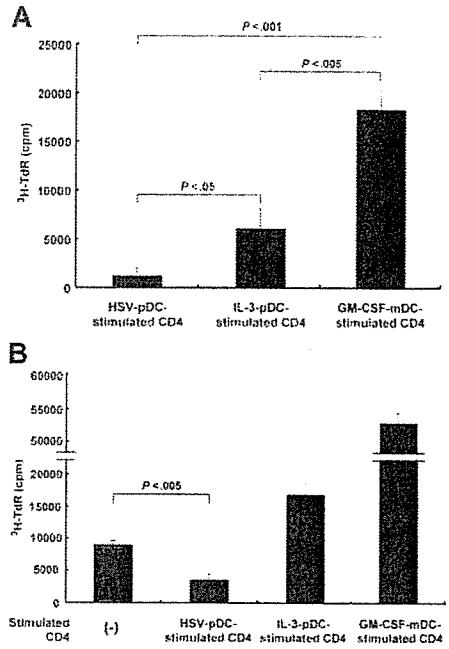

Figure 3. HSV-pDCs induce anergic and regulatory CD4$^+$ T cells. (A) Naive CD4$^+$ T cells stimulated with allogeneic DCs for 8 days were restimulated with irradiated allogeneic CD3-depleted PBMCs. After 4 days, wells were pulsed for 16 hours with [^{3}H] thymidine. (B) Naive CD4$^+$ T cells were stimulated with irradiated allogeneic CD3-depleted PBMCs in the absence or presence of CD4$^+$ T cells that had been stimulated with one of the 3 types of DCs. After 4 days, wells were pulsed for 16 hours with [^{3}H] thymidine. Error bars indicate SD. The data shown are representative of 3 experiments.

originally cocultured with HSV-pDCs showed markedly reduced proliferation after restimulation. CD4$^+$ T cells originally cocultured with IL-3–pDCs proliferated significantly more than T cells originally cocultured with HSV-pDCs ($P < .05$), but significantly less than T cells cocultured with GM-CSF–mDCs ($P < .005$). CD4$^+$ T cells originally cocultured with GM-CSF–mDCs vigorously proliferated after restimulation. These data indicate that HSV-pDCs, and to a lesser extent IL-3–pDCs, induce CD4$^+$ T-cell anergy.

Next, we examined whether the anergic CD4$^+$ T cells have a regulatory activity, that is, whether they suppress proliferation of coexisting T cells. We cocultured naive CD4$^+$ T cells and DC-primed CD4$^+$ T cells from the same donor, in the presence of PBMCs from the same donor as that of DCs for 5 days, and measured [^{3}H] thymidine incorporation during the last 16 hours. As shown in Figure 3B, naive CD4$^+$ T cells stimulated with allogeneic PBMCs, in the absence of DC-stimulated CD4$^+$ T cells, exhibited moderate proliferation. This proliferation was significantly suppressed by coexisting CD4$^+$ T cells stimulated with HSV-pDCs ($P < .005$). In contrast, CD4$^+$ T cells stimulated with IL-3–pDCs or GM-CSF–mDCs did not show such suppressive activity. This indicates that CD4$^+$ T cells stimulated with HSV-pDCs, but not those stimulated with IL-3–pDCs or GM-CSF–mDCs, have regulatory as well as anergic properties.

The induction of anergic and regulatory properties of CD4$^+$ T cells is dependent on type I IFNs and IL-10

It has been shown that polyclonal stimulation of naive CD4$^+$ T cells in the presence of IFN-α and IL-10 induces anergic and regulatory T cells.[18] Thus, we asked whether type I IFNs derived from HSV-pDCs and IL-10 derived from CD4$^+$ T cells themselves are responsible for the induction of anergic and regulatory properties of the T cells. We added blocking anti-IFN-α/β receptor mAb or anti-IL-10 mAb to the coculture of HSV-pDCs and allogeneic naive CD4$^+$ T cells, and restimulated the T cells with PBMCs from the same donor as that of DCs for 5 days, and measured [^{3}H] thymidine incorporation during the last 16 hours. As shown in Figure 4A, the addition of blocking anti-IFN-α/β receptor mAb or anti-IL-10 mAb during primary culture diminished the induction of anergy. The addition of a mixture of anti-IFN-α/β receptor mAb and anti-IL-10 mAb did not show an additive effect. Thus, both pDC-derived type I IFNs and T cell-derived IL-10[15] present during priming are responsible for the induction of CD4$^+$ T-cell anergy by HSV-pDCs.

Next, we examined whether type I IFNs and IL-10 are also responsible for the induction of regulatory T cells. We stimulated allogeneic naive CD4$^+$ T cells with HSV-pDCs in the presence or absence of anti-IFN-α/β receptor mAb or anti-IL-10 mAb. Thereafter, we cocultured naive CD4$^+$ T cells and HSV-pDC–stimulated CD4$^+$ T cells from the same donor, in the presence of PBMCs from the same donor as that of pDCs. Inhibition of type I IFNs or IL-10 during the priming of naive CD4$^+$ T cells with HSV-pDCs significantly reduced the generation of regulatory T cells (Figure 4B). The addition of a mixture of anti-IFN-α/β receptor mAb and anti-IL-10 mAb did not show an additive effect. Thus, both pDC-derived type I IFNs and T cell–derived IL-10 present during priming are responsible for the induction of regulatory T cells.

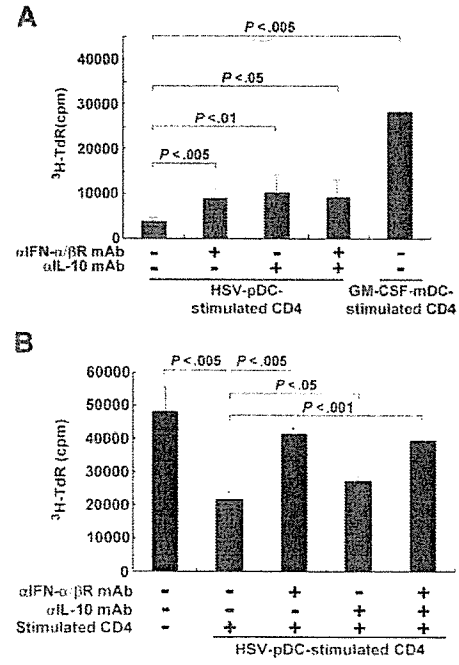

Figure 4. The induction of anergic and regulatory properties of CD4$^+$ T cells is dependent on type I IFNs and IL-10. (A) Naive CD4$^-$ T cells were stimulated with allogeneic HSV-pDCs for 8 days in the presence of isotype-matched control mAb, anti-IFN-α/β receptor mAb, anti-IL-10 mAb, or a mixture of the both mAbs. Alternatively, T cells were stimulated with allogeneic GM-CSF–mDCs for comparison. The CD4$^-$ T cells were harvested and restimulated with irradiated allogeneic CD3-depleted PBMCs. After 4 days, wells were pulsed for 16 hours with [^{3}H] thymidine. (B) Naive CD4$^-$ T cells were stimulated with allogeneic HSV-pDCs for 8 days in the presence of isotype-matched control mAb, anti-IFN-α/β receptor mAb, anti-IL-10 mAb, or a mixture of the both mAbs. Naive CD4$^-$ T cells were stimulated with irradiated allogeneic CD3-depleted PBMCs in the absence or presence of the CD4$^-$ T cells that had been stimulated with HSV-pDCs. After 4 days, wells were pulsed for 16 hours with [^{3}H] thymidine. Error bars indicate SD. The data shown are representative of 3 experiments.

HSV-pDCs and IL-3–pDCs induce granzymes and perforin in CD4+ T cells in a partially IL-10–dependent manner

It has recently been shown that anti-CD3/anti-CD46 stimulation induces CD4+ regulatory T cells that express granzymes and perforin.[21,22] Because perforin has been shown to play an important role in down-regulating T-cell responses in chronic viral infection,[20] we examined whether HSV-pDCs induce the expression of granzymes and perforin in naive CD4+ T cells. We cocultured allogeneic naive CD4+ T cells with HSV-pDCs, IL-3–pDCs, or GM-CSF–mDCs for 8 days in the presence or absence of anti-IFN-α/β receptor mAb or anti-IL-10 mAb, and examined the expression of granzyme A, granzyme B, and perforin by intracellular staining. Unstimulated naive CD4+ T cells did not express detectable levels of granzyme A, granzyme B, or perforin (data not shown). As shown in Figure 5, granzyme A was induced by stimulation with any DCs: HSV-pDCs, IL-3–pDCs, and GM-CSF–mDCs. HSV-pDCs, and to a lesser extent IL-3–pDCs, induced high levels of granzyme B in CD4+ T cells, whereas GM-CSF–mDCs induced only a low level of granzyme B. HSV-pDCs, and to a lesser extent IL-3–pDCs, induced moderate levels of perforin, whereas GM-CSF–mDCs did not induce a significant level of perforin. The induction of granzyme A or granzyme B by HSV-pDCs did not diminish in the presence of anti-IFN-α/β receptor mAb, whereas the induction of perforin moderately diminished. The induction of the 3 molecules by HSV-pDCs or IL-3–pDCs partially but substantially diminished in the presence of anti-IL-10 mAb. These data indicate that HSV-pDCs and to a lesser extent IL-3–pDCs, but not GM-CSF–mDCs, induce CD4+ T cells to express granzyme B and perforin in a partially IL-10–dependent manner. Type I IFNs may also be involved in the induction of perforin.

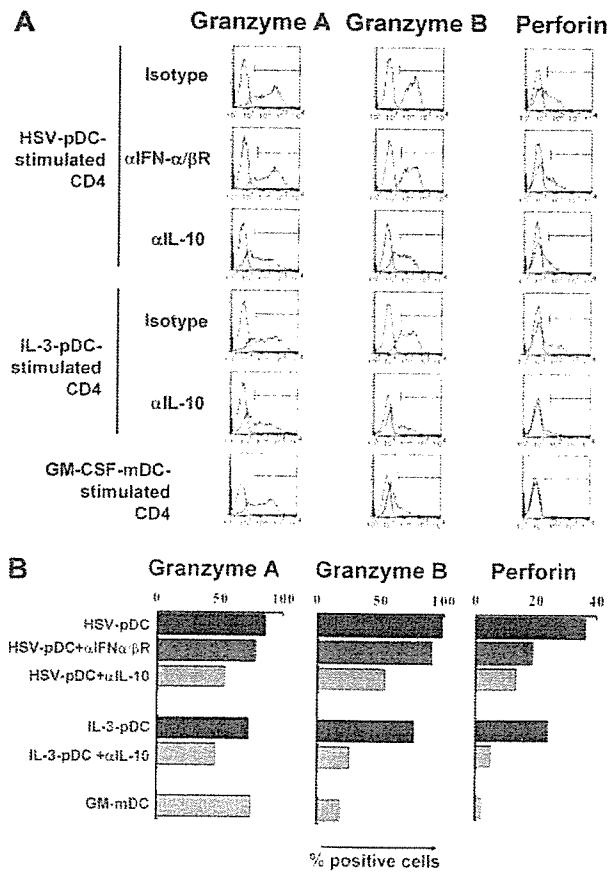

Figure 5. HSV-pDCs and IL-3–pDCs induce granzymes and perforin in CD4+ T cells in a partially IL-10–dependent manner. Naive CD4+ T cells were stimulated with allogeneic HSV-pDCs or IL-3–pDCs for 8 days in the presence of isotype-matched control mAb, anti-IFN-α/β receptor mAb, or anti-IL-10 mAb. Alternatively, T cells were stimulated with allogeneic GM-CSF–mDCs for comparison. Activated T cells were gated based on the expression of CD25, and expression of intracellular granzyme A, granzyme B, and perforin was analyzed by flow cytometry. (A) Histograms. Open histograms represent cells stained with isotype-matched control mAbs. (B) Percentages of cells expressing the 3 molecules, indicated with markers in panel A. The data shown are representative of 3 experiments.

CD4+ T cells stimulated with HSV-pDCs exhibit perforin-dependent cytotoxicity

Finally, we examined whether CD4+ T cells stimulated with the 3 types of DCs have cytotoxic activity in accordance with the expression of granzymes and perforin. We used a Burkitt lymphoma cell line Daudi or a myelomonocytic cell line U937 as target cells of cytotoxicity assay. We stained the target cells with CFSE[22] and cocultured the effector and target cells for 4 hours. Then the percentages of killed CFSE-labeled target cells were calculated by staining them with 7-AAD. As shown in Figure 6A, a large proportion of Daudi cocultured with HSV-pDC–stimulated CD4+ T cells underwent apoptosis. Daudi cocultured with IL-3/pDC-stimulated CD4+ T cells also underwent apoptosis, albeit to a lesser extent. The extent of apoptosis in both conditions was correlated with E/T ratios. In contrast, Daudi cocultured with GM-CSF/mDC-stimulated CD4+ T cells minimally underwent apoptosis. The apoptosis induced by HSV-pDC–stimulated CD4+ T cells was substantially diminished by the addition of EGTA, indicating that the death was perforin-dependent (Figure 6B). The apoptosis induced by IL-3-pDC–stimulated CD4+ T cells was marginally inhibited by EGTA. We obtained similar results using U937 as target cells (data not shown). As target cells, we also used activated T cells from the same donors as DC donors (allospecific targets), or activated T cells from donors different from DC and effector T-cell donors (third-party targets). Third-party target T cells (Figure 6C) as well as allospecific target T cells (data not shown) were substantially killed by HSV-pDC–stimulated CD4+ T cells and were also killed by IL-3–pDC–stimulated CD4+ T cells to a lesser extent, whereas the killing by GM-CSF–mDC–stimulated CD4+ T cells was minimal, as observed in the killing of unrelated tumor cell lines. These data indicate that in proportion to the degree of up-regulation of granzymes and perforin, CD4+ T cells stimulated with HSV-pDCs have the strongest perforin-dependent cytotoxic activity among the 3 CD4+ T cells stimulated with different DCs in an antigen-nonspecific manner. CD4+ T cells stimulated with IL-3–pDCs may also have a significant cytotoxicity.

Discussion

During immune responses to microbial pathogens, overwhelming pathologic immune reactions need to be avoided to minimize tissue damage. IFN-γ/IL-10–producing CD4+ T cells have been recognized in infections by several pathogens,[2,4-6] and may play an important role in down-modulating pathologic immune reactions and may also be responsible for allowing persistent infection.[2,3,7,29] Given that the direction of naive CD4+ T-cell differentiation is largely determined by the subset and activation state of DCs, it is important to elucidate which type of DCs induces naive CD4+ T cells to differentiate into immunoregulatory IFN-γ/IL-10–producing T cells during infection. Here we showed that the IFN-γ/IL-10–producing CD4+ T cells induced by HSV-pDCs

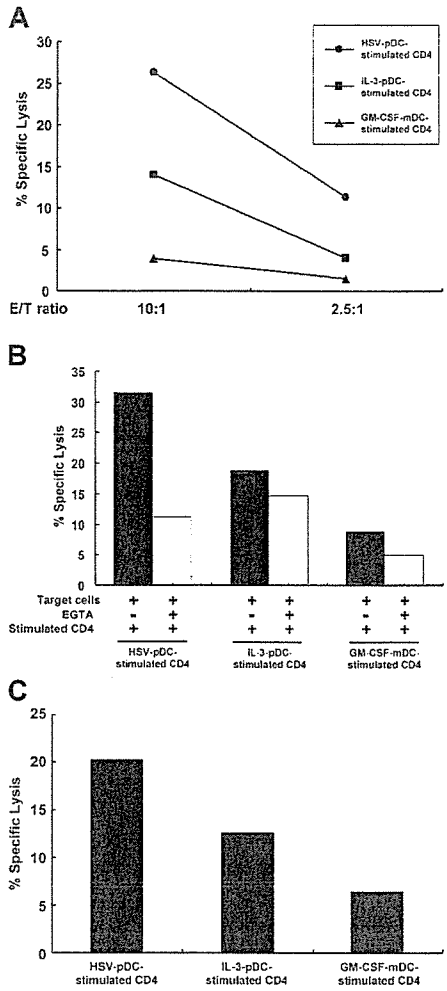

Figure 6. CD4⁺ T cells stimulated with HSV-pDCs exhibit perforin-dependent cytotoxicity. (A) Naive CD4⁺ T cells stimulated with the 3 types of allogeneic DCs for 8 days (effector cells) were cocultured with CFSE-labeled Daudi target cells at an E/T ratio of 10:1 or 2.5:1 for 4 hours. Immediately before analysis, 7-AAD was added to each sample, and percentages of 7-AAD⁺ cells were analyzed by flow cytometry. Basal lysis of the target cells was 9.6%. The data shown are representative of 2 experiments. (B) Naive CD4⁺ T cells stimulated with the 3 types of allogeneic DCs for 8 days (effector cells) were cocultured with CFSE-labeled Daudi target cells at an E/T ratio of 30:1 for 4 hours in the absence or presence of EGTA. Percentages of 7-AAD⁺ cells were analyzed by flow cytometry as shown in panel A. Basal lysis of the target cells was 18%. Filled and open bars represent percent specific lysis induced in the absence or presence of EGTA, respectively. The data shown are representative of 3 experiments. (C) Naive CD4⁺ T cells stimulated with the 3 types of allogeneic DCs for 8 days (effector cells) were cocultured with CFSE-labeled activated T cells from third-party donors (target cells) at an E/T ratio of 30:1 for 4 hours. Percentages of 7-AAD⁺ cells were analyzed by flow cytometry as shown in panel A. Basal lysis of the target cells was 16%. The data shown are representative of 2 experiments.

acquire anergic and regulatory properties by the action of pDC-derived type I IFNs and T cell–derived IL-10. Interestingly, cytotoxic molecules perforin and granzyme B in CD4⁺ T cells are induced by pDCs in an IL-10–dependent manner. These results suggest an immunoregulatory role of type I IFN-producing pDCs through the induction of perforin/granzyme-expressing regulatory CD4⁺ T cells and present a possible mechanism by which pDCs induce coordinated antiviral immunity by preventing excessive immune responses.

Several studies have shown that pDCs are capable of inducing immunoregulatory T cells through various mechanisms. For example, pDC precursors induce CD4⁺ T-cell anergy, apparently due to the lack of costimulatory molecules.[30] IL-3/CD40L-stimulated pDCs induce IL-10–producing CD8⁺ regulatory T cells.[31] pDCs stimulated with CpG ODNs induce Foxp3-expressing CD4⁺CD25⁺ regulatory T cells.[32] Mouse in vivo studies have shown that lung pDCs prevent asthmatic reactions to harmless inhaled antigens by inducing regulatory T cells.[33] pDC precursors contained in the graft facilitate allogeneic hematopoietic stem cell engraftment.[34] These findings indicate that pDC precursors that express low levels of costimulatory molecules or pDCs activated with particular stimulations are capable of inducing anergic or regulatory T cells. However, these studies do not ascribe the induction of T-cell suppression to type I IFNs. Here we show the importance of type I IFNs in inducing anergic and regulatory T cells by pDCs under the conditions where viral stimuli induce them to produce the cytokines. Although murine pDCs have been shown to induce anergic T cells through the expression of indoleamine 2,3-dioxygenase (IDO),[35,36] the addition of an IDO inhibitor 1-methyl-D-tryptophan to the coculture of pDCs and naive CD4⁺ T cells did not inhibit the induction of regulatory T cells (unpublished data, September 2004), indicating that IDO is not involved in the system shown in this study.

Recent studies have been revealing an immunoregulatory role of type I IFNs through different mechanisms. First, IFN-α treatment of naive CD4⁺ T cells delays their entry into cell cycle early on T-cell receptor (TCR) triggering and sensitizes T cells to activation-induced cell death later after activation.[37,38] These mechanisms may explain the markedly suppressed proliferation of naive CD4⁺ T cells stimulated with type I IFN-producing HSV-pDCs. The attenuated proliferation of CD4⁺ T cells stimulated with virus-activated pDCs may result in accumulation of IFN-γ/IL-10–producing regulatory CD4⁺ T cells at a chronic stage during viral infection.

Second, type I IFNs have been shown to induce CD4⁺ T cells that produce IL-10 together with IFN-γ. For example, polyclonal stimulation of human naive CD4⁺ T cells using anti-CD3 mAb in the presence of IFN-α induce IFN-γ/IL-10–producing CD4⁺ T cells that have regulatory activity.[18,39] Type I IFN receptor-deficient mice generate reduced numbers of IL-10–producing CD4⁺ T cells, which correlates with enhancement of CD8⁺ T-cell responses, suggesting that type I IFNs suppress CD8⁺ T-cell responses through the induction of IL-10–producing CD4⁺ regulatory T cells.[19] The present study suggests that type I IFN-producing pDCs may be the APCs responsible for the induction of type I IFN-dependent CD4⁺ regulatory T cells.

IFN-γ/IL-10–producing CD4⁺ T cells are identified in hosts suffering from chronic or persistent infections with various types of pathogens.[2,4-6] Such T cells have been suggested to be responsible for permitting persistent infection.[2] In addition, IL-10–producing CD4⁺ regulatory T cells generated in mice with retroviral infection have been shown to contribute to viral persistence.[40] These IL-10–producing T cells may also play an important role in preventing excessive immune responses, as the absence of IL-10 leads to uncontrolled lethal immune responses.[1] An important question is what types of DCs induce immunoregulatory IFN-γ/IL-10–producing CD4⁺ T cells frequently identified in infected hosts. In mice, it has been shown that IL-12/IL-10–producing CD8α⁺ DCs stimulated with heat-killed *Listeria* induce IFN-γ⁻IL-10⁺ regulatory CD4⁺ T cells that inhibit airway hyperreactivity.[41] IL-12 has been shown to induce human CD4⁺ T cells to produce IL-10 together with IFN-γ.[5,42] In humans, mDCs produce IL-12 but not IFN-α in response to bacterial stimuli, whereas pDCs produce IFN-α but not IL-12 in response to viral stimuli.[10,15] Therefore, in humans, IL-12–producing mDCs may induce immunoregulatory

IFN-γ/IL-10–producing $CD4^+$ T cells in bacterial infections as shown in mice with $CD8\alpha^+$ DCs,[41] whereas IFN-α–producing pDCs may induce such T cells in persistent infections with viruses such as HSV and hepatitis C virus.[6]

It has been shown that naturally occurring $CD4^+CD25^+$ regulatory T cells[43,44] as well as IL-10–producing "adaptive" regulatory T cells in some cases[19,41] highly express *FOXP3* mRNA. Thus, we examined by real-time reverse transcription-polymerase chain reaction (RT-PCR) whether HSV-pDCs specifically induce the expression of *FOXP3* mRNA in naive $CD4^+$ T cells. Naive $CD4^+$ T cells stimulated with HSV-pDCs, IL-3–pDCs, or GM-CSF–mDCs for 8 days expressed comparable levels of *FOXP3* mRNA, which were about half of the *FOXP3* levels in $CD4^+CD25^+$ T cells isolated from adult PBMCs (data not shown). Thus, *FOXP3* mRNA is not specifically induced in $CD4^+$ T cells stimulated with HSV-pDCs and does not appear to be important in regulatory activity of such T cells.

An increase in perforin-expressing $CD4^+$ T cells has been observed in patients with chronic viral infections, suggesting a physiologic role of such T cells in antiviral immune responses.[45] Because activated $CD8^+$ T cells that cause tissue damage accumulate in perforin-deficient mice during chronic viral infection,[20] perforin-mediated autologous cell killing appears to be important in avoiding pathologic immune reactions. Furthermore, stimulation of naive $CD4^+$ T cells with anti-CD3 and anti-CD46 mAbs has been shown to induce them to differentiate into granzymes/perforin$^+$ IL-10–producing regulatory T cells[29] that kill allogeneic cells[22] as well as autologous immune cells.[21] These findings suggest that $CD4^+$ T cells positive for granzymes/perforin play an important immunoregulatory role in chronic viral infections by killing pathogenic immune cells. However, the previous studies did not address the type of APCs responsible for inducing regulatory $CD4^+$ cytotoxic T lymphocytes (CTLs). Here we propose that virus-stimulated pDCs are such APCs that keep antiviral immune responses at an appropriate level by inducing regulatory $CD4^+$ CTLs. Because IL-3–stimulated pDCs are also capable of inducing $CD4^+$ T cells positive for granzymes/perforin, pDCs may generate regulatory $CD4^+$ CTLs in immune responses other than antiviral ones. The involvement of endogenous IL-10 in inducing the expression of granzymes and perforin was unexpected. IL-10 has been shown to enhance cytotoxic activity of natural killer cells and CTLs, although the expression of granzymes and perforin was not investigated in these studies.[46,47] Thus, $CD4^+$ T cells stimulated with pDCs may play an immunoregulatory role in chronic antiviral immune responses by expressing granzymes and perforin in an IL-10–dependent manner. The moderate reduction of perforin expression by anti-IFN-α/β receptor mAb also suggests the involvement of type I IFNs in the induction of perforin. Apparent lack of antigen specificity or allospecificity of the cytotoxicity in the previous[21] and present studies, together with generalized and uncontrolled activation of T cells and macrophages in individuals with perforin gene defects,[48] suggests importance of the perforin pathway in the maintenance of general immune homeostasis.

In summary, type I IFN-producing, virus-stimulated pDCs may play a dual role during the course of antiviral immune responses. Immediately after viral invasion, pDCs play a pivotal role in provoking antiviral innate immunity by producing a vast amount of type I IFNs. Thereafter, type I IFN-producing pDCs may downmodulate antiviral adaptive immune responses by inducing granzymes/perforin-positive, IFN-γ/IL-10^+ $CD4^+$ regulatory T cells. The present study adds another novel function to the versatile immune cell type, pDCs, that is, the induction of $CD4^+$ cytotoxic regulatory T cells.

Acknowledgments

We thank Drs Masaki Yasukawa and Tetsushi Yoshikawa for providing HSV-1 (KOS strain) and Keiko Fukunaga for her excellent technical assistance.

References

1. Gazzinelli RT, Wysocka M, Hieny S, et al. In the absence of endogenous IL-10, mice acutely infected with *Toxoplasma gondii* succumb to a lethal immune response dependent on $CD4^+$ T cells and accompanied by overproduction of IL-12, IFN-gamma and TNF-alpha. J Immunol. 1996;157:798-805.
2. Belkaid Y, Hoffmann KF, Mendez S, et al. The role of interleukin (IL)-10 in the persistence of *Leishmania major* in the skin after healing and the therapeutic potential of anti-IL-10 receptor antibody for sterile cure. J Exp Med. 2001;194:1497-1506.
3. Belkaid Y, Piccirillo CA, Mendez S, Shevach EM, Sacks DL. $CD4^+CD25^+$ regulatory T cells control *Leishmania major* persistence and immunity. Nature. 2002;420:502-507.
4. Gerosa F, Nisii C, Righetti S, et al. CD4(+) T cell clones producing both interferon-gamma and interleukin-10 predominate in bronchoalveolar lavages of active pulmonary tuberculosis patients. Clin Immunol. 1999;92:224-234.
5. Pohl-Koppe A, Balashov KE, Steere AC, Logigian EL, Hafler DA. Identification of a T cell subset capable of both IFN-gamma and IL-10 secretion in patients with chronic Borrelia burgdorferi infection. J Immunol. 1998;160:1804-1810.
6. MacDonald AJ, Duffy M, Brady MT, et al. CD4 T helper type 1 and regulatory T cells induced against the same epitopes on the core protein in hepatitis C virus-infected persons. J Infect Dis. 2002;185:720-727.
7. Mendez S, Reckling SK, Piccirillo CA, Sacks D, Belkaid Y. Role for $CD4^+$ $CD25^+$ regulatory T cells in reactivation of persistent leishmaniasis and control of concomitant immunity. J Exp Med. 2004;200:201-210.
8. Banchereau J, Briere F, Caux C, et al. Immunobiology of dendritic cells. Annu Rev Immunol. 2000; 18:767-811.
9. Ito T, Liu YJ, Kadowaki N. Functional diversity and plasticity of human dendritic cell subsets. Int J Hematol. 2005;81:188-196.
10. Kadowaki N, Ho S, Antonenko S, et al. Subsets of human dendritic cell precursors express different Toll-like receptors and respond to different microbial antigens. J Exp Med. 2001;194:863-870.
11. Muller U, Steinhoff U, Reis LF, et al. Functional role of type I and type II interferons in antiviral defense. Science. 1994;264:1918-1921.
12. Cella M, Jarrossay D, Facchetti F, et al. Plasmacytoid monocytes migrate to inflamed lymph nodes and produce large amounts of type I interferon. Nat Med. 1999;5:919-923.
13. Fonteneau J-F, Gilliet M, Larsson M, et al. Activation of influenza virus-specific $CD4^+$ and $CD8^+$ T cells: a new role for plasmacytoid dendritic cells in adaptive immunity. Blood. 2003;101:3520-3526.
14. Schlecht G, Garcia S, Escriou N, Freitas AA, Leclerc C, Dadaglio G. Murine plasmacytoid dendritic cells induce effector/memory $CD8^+$ T-cell responses in vivo after viral stimulation. Blood. 2004;104:1808-1815.
15. Kadowaki N, Antonenko S, Lau JY, Liu YJ. Natural interferon alpha/beta-producing cells link innate and adaptive immunity. J Exp Med. 2000; 192:219-226.
16. Pfeffer LM, Dinarello CA, Herberman RB, et al. Biological properties of recombinant alpha-interferons: 40th anniversary of the discovery of interferons. Cancer Res. 1998;58:2489-2499.
17. Manca C, Tsenova L, Bergtold A, et al. Virulence of a Mycobacterium tuberculosis clinical isolate in mice is determined by failure to induce Th1 type immunity and is associated with induction of IFN-alpha /beta PNAS. 2001:98:5752-5757.
18. Levings MK, Sangregorio R, Galbiati F, Squadrone S, de Waal Malefyt R, Roncarolo MG. IFN-alpha and IL-10 induce the differentiation of human type 1 T regulatory cells. J Immunol. 2001; 166:5530-5539.
19. Dikopoulos N, Bertoletti A, Kroger A, Hauser H, Schirmbeck R, Reimann J. Type I IFN negatively regulates $CD8^+$ T cell responses through IL-10-producing $CD4^+$ T regulatory 1 cells. J Immunol. 2005;174:99-109.
20. Matloubian M, Suresh M, Glass A, et al. A role for perforin in downregulating T-cell responses during chronic viral infection. J Virol. 1999;73:2527-2536.
21. Grossman WJ, Verbsky JW, Barchet W, Colonna M, Atkinson JP, Ley TJ. Human T regulatory cells can use the perforin pathway to cause autologous target cell death. Immunity. 2004;21:589-601.

22. Grossman WJ, Verbsky JW, Tollefsen BL, Kemper C, Atkinson JP, Ley TJ. Differential expression of granzymes A and B in human cytotoxic lymphocyte subsets and T regulatory cells. Blood. 2004;104:2840-2848.
23. Krug A, Rothenfusser S, Hornung V, et al. Identification of CpG oligonucleotide sequences with high induction of IFN-alpha/beta in plasmacytoid dendritic cells. Eur J Immunol. 2001;31:2154-2163.
24. Bacchetta R, Sartirana C, Levings MK, Bordignon C, Narula S, Roncarolo MG. Growth and expansion of human T regulatory type 1 cells are independent from TCR activation but require exogenous cytokines. Eur J Immunol. 2002;32:2237-2245.
25. Rissoan M-C, Soumelis V, Kadowaki N, et al. Reciprocal control of T helper cell and dendritic cell differentiation. Science. 1999;283:1183-1186.
26. Lecoeur H, Fevrier M, Garcia S, Riviere Y, Gougeon ML. A novel flow cytometric assay for quantitation and multiparametric characterization of cell-mediated cytotoxicity. J Immunol Methods. 2001;253:177-187.
27. Lund J, Sato A, Akira S, Medzhitov R, Iwasaki A. Toll-like receptor 9-mediated recognition of herpes simplex virus-2 by plasmacytoid dendritic cells. J Exp Med. 2003;198:513-520.
28. Groux H, O'Garra A, Bigler M, et al. A CD4$^+$ T-cell subset inhibits antigen-specific T-cell responses and prevents colitis. Nature. 1997;389:737-742.
29. Kemper C, Chan AC, Green JM, Brett KA, Murphy KM, Atkinson JP. Activation of human CD4$^+$ cells with CD3 and CD46 induces a T-regulatory cell 1 phenotype. Nature. 2003;421:388-392.
30. Kuwana M, Kaburaki J, Wright TM, Kawakami Y, Ikeda Y. Induction of antigen-specific human CD4(+) T cell anergy by peripheral blood DC2 precursors. Eur J Immunol. 2001;31:2547-2557.
31. Gilliet M, Liu Y-J. Generation of human CD8 T regulatory cells by CD40 ligand-activated plasmacytoid dendritic cells. J Exp Med. 2002;195:695-704.
32. Moseman EA, Liang X, Dawson AJ, et al. Human plasmacytoid dendritic cells activated by CpG oligodeoxynucleotides induce the generation of CD4$^+$CD25$^+$ regulatory T cells. J Immunol. 2004;173:4433-4442.
33. de Heer HJ, Hammad H, Soullie T, et al. Essential role of lung plasmacytoid dendritic cells in preventing asthmatic reactions to harmless inhaled antigen. J Exp Med. 2004;200:89-98.
34. Fugier-Vivier IJ, Rezzoug F, Huang Y, et al. Plasmacytoid precursor dendritic cells facilitate allogeneic hematopoietic stem cell engraftment. J Exp Med. 2005;201:373-383.
35. Munn DH, Sharma MD, Hou D, et al. Expression of indoleamine 2,3-dioxygenase by plasmacytoid dendritic cells in tumor-draining lymph nodes. J Clin Invest. 2004;114:280-290.
36. Fallarino F, Asselin-Paturel C, Vacca C, et al. Murine plasmacytoid dendritic cells initiate the immunosuppressive pathway of tryptophan catabolism in response to CD200 receptor engagement. J Immunol. 2004;173:3748-3754.
37. Dondi E, Rogge L, Lutfalla G, Uze G, Pellegrini S. Down-modulation of responses to type I IFN upon T cell activation. J Immunol. 2003;170:749-756.
38. Dondi E, Roue G, Yuste VJ, Susin SA, Pellegrini S. A dual role of IFN-alpha in the balance between proliferation and death of human CD4$^+$ T lymphocytes during primary response. J Immunol. 2004;173:3740-3747.
39. Demeure CE, Wu CY, Shu U, et al. In vitro maturation of human neonatal CD4 T lymphocytes, II: cytokines present at priming modulate the development of lymphokine production. J Immunol. 1994;152:4775-4782.
40. Dittmer U, He H, Messer RJ, et al. Functional impairment of CD8(+) T cells by regulatory T cells during persistent retroviral infection. Immunity. 2004;20:293-303.
41. Stock P, Akbari O, Berry G, Freeman GJ, Dekruyff RH, Umetsu DT. Induction of T helper type 1-like regulatory cells that express Foxp3 and protect against airway hyper-reactivity. Nat Immunol. 2004;5:1149-1156.
42. Gerosa F, Paganin C, Peritt D, et al. Interleukin-12 primes human CD4 and CD8 T cell clones for high production of both interferon-gamma and interleukin-10. J Exp Med. 1996;183:2559-2569.
43. Hori S, Nomura T, Sakaguchi S. Control of regulatory T cell development by the transcription factor Foxp3. Science. 2003;299:1057-1061.
44. Yagi H, Nomura T, Nakamura K, et al. Crucial role of FOXP3 in the development and function of human CD25+CD4+ regulatory T cells. Int Immunol. 2004;16:1643-1656.
45. Appay V, Zaunders JJ, Papagno L, et al. Characterization of CD4(+) CTLs ex vivo. J Immunol. 2002;168:5954-5958.
46. Cai G, Kastelein RA, Hunter CA. IL-10 enhances NK cell proliferation, cytotoxicity and production of IFN-gamma when combined with IL-18. Eur J Immunol. 1999;29:2658-2665.
47. Takayama T, Tahara H, Thomson AW. Differential effects of myeloid dendritic cells retrovirally transduced to express mammalian or viral interleukin-10 on cytotoxic T lymphocyte and natural killer cell functions and resistance to tumor growth. Transplantation. 2001;71:1334-1340.
48. Stepp SE, Dufourcq-Lagelouse R, Le Deist F, et al. Perforin gene defects in familial hemophagocytic lymphohistiocytosis. Science. 1999;286:1957-1959.

Molecular basis of clonal expansion of hematopoiesis in 2 patients with paroxysmal nocturnal hemoglobinuria (PNH)

Norimitsu Inoue, Tomohisa Izui-Sarumaru, Yoshiko Murakami, Yuichi Endo, Jun-Ichi Nishimura, Ken Kurokawa, Maki Kuwayama, Hiroaki Shime, Takashi Machii, Yuzuru Kanakura, Gabrielle Meyers, Carl Wittwer, Zhong Chen, William Babcock, Debra Frei-Lahr, Charles J. Parker, and Taroh Kinoshita

Somatic mutation of *PIGA* in hematopoietic stem cells causes deficiency of glycosyl phosphatidylinositol–anchored proteins in paroxysmal nocturnal hemoglobinuria (PNH) that underlies the intravascular hemolysis but does not account for expansion of the PNH clone. Immune mechanisms may mediate clonal selection but appear insufficient to account for the clonal dominance necessary for PNH to become clinically apparent. Herein, we report 2 patients with PNH whose *PIGA*-mutant cells had a concurrent, acquired rearrangement of chromosome 12. In both cases, der(12) had a break within the 3′ untranslated region of *HMGA2*, the architectural transcription factor gene deregulated in many benign mesenchymal tumors, that caused ectopic expression of *HMGA2* in the bone marrow. These observations suggest that aberrant *HMGA2* expression, in concert with mutant *PIGA*, accounts for clonal hematopoiesis in these 2 patients and suggest the concept of PNH as a benign tumor of the bone marrow. (Blood. 2006;108:4232-4236)

Introduction

Paroxysmal nocturnal hemoglobinuria (PNH) is a consequence of nonmalignant clonal expansion of hematopoietic stem cells with somatic mutation of *PIGA*.[1] Mutant *PIGA*[2] explains the deficiency of glycosyl phosphatidylinositol–anchored proteins (GPI-APs) that underlies the intravascular hemolysis of PNH.[3] However, *PIGA*-mutant stem cells have no intrinsic proliferative advantage,[4,5] suggesting a 2-step model of pathogenesis.

Step 1 of this model, clonal selection,[6,7] is envisioned as a conditional survival advantage that depends on deficiency of 1 or more GPI-APs. The close association of PNH with aplastic anemia, suggests that the selection pressure is immune mediated.[6,7] But, although 60% to 70% of patients with aplastic anemia have small, subclinical populations of GPI-AP$^-$ hematopoietic cells at diagnosis,[8] only 10% to 15% subsequently develop clinically apparent PNH.[9] In the remainder, GPI-AP$^-$ cells persist subclinically or disappear,[8] suggesting that mutant *PIGA* (and the consequent deficiency of GPI-APs) is necessary for clonal selection but is insufficient to account for the clonal expansion required for clinical manifestations of PNH to become apparent.

Clonal expansion, step 2 of the PNH pathogenesis model, is envisioned as a consequence of clonal evolution in which a second somatic mutation bestows on the *PIGA*-mutant stem cell a proliferative advantage.[10] Herein, we present evidence supporting this 2-step model by showing a concurrent, acquired genetic abnormality in the *PIGA*-mutant cells of 2 patients that establishes a novel mechanism for the nonmalignant clonal hematopoieis characteristic of PNH.

Patients, materials, and methods

Patients

Informed consent was obtained from patients J20 and US1 according to protocols approved by the Institutional Review Boards of Osaka University Hospital (Osaka, Japan) and the University of Utah School of Medicine (Salt Lake City, UT), respectively.

Hybrid cell lines

Monocytes derived from J20 or US1 were fused with the hypoxanthine phosphoribosyltransferase–negative mouse myeloma cell line, P3-X63-Ag8.653, as previously described.[11] Lines carrying human chromosome 12 were selected by analyses of expression of both CD9 and polymorphic markers *D12S77* and *D12S78*. The B-lymphoblastoid cell line JY25[12] was used as a control in some experiments.

From the Department of Molecular Genetics, Osaka Medical Center for Cancer, Japan; the Department of Immunoregulation, Research Institute for Microbial Diseases, Osaka University, Japan; the Department of Immunology, Fukushima Medical University, Japan; the Department of Medicine, Duke University Medical Center, Durham, NC; the Genome Information Research Center, Osaka University, Japan; the Department of Hematology and Oncology, Osaka University School of Medicine, Japan; the Department of Medicine, Division of Hematology and Bone Marrow Transplant, University of Utah School of Medicine, Salt Lake City, UT; the Department of Medicine, Hematology/Oncology Section, George E. Whalen Veterans Administration (VA) Medical Center, Salt Lake City, UT; the Department of Pathology, University of Utah School of Medicine, Salt Lake City, UT; the Division of Medical Genetics, Department of Pediatrics, University of Utah School of Medicine, Salt Lake City, UT; the Department of Medicine, Division of Hematology/Oncology, Baptist Medical Center, Columbia, SC; the Department of Medicine, Division of Hematology, Medical University of South Carolina, Charleston, SC; and the Core Research for Evolutional Science and Technology, Japan Science and Technology Agency, Saitama, Japan.

Submitted May 23, 2006; accepted August 8, 2006. Prepublished online as *Blood* First Edition Paper, August 29, 2006; DOI 10.1182/blood-2006-05-025148.

An Inside *Blood* analysis of this article appears at the front of this issue.

The publication costs of this article were defrayed in part by page charge payment. Therefore, and solely to indicate this fact, this article is hereby marked "advertisement" in accordance with 18 USC section 1734.

Determination of chromosomal breakpoints

Initial mapping of breakpoints required a combination of polymerase chain reaction (PCR), inverse PCR, and Southern blotting. For fine mapping, sequence-tagged site markers were generated by PCR using primers based on sequences of ends of bacterial artificial chromosome (BAC) clones or on data in the human genome database of the National Center for Biotechnical Information. GenBank accession numbers of BAC clones (CHORI BACPAC Resource Center) are as follows: RP11-425I22 (425I22), AC074030; RP11-471G7 (471G7), AC024935; RP11-150C16 (150C16), AC046129; RP11-366L20 (366L20), AC090673; RP11-474P2, AC025031; RP11-221N13, AC090023; RP11-434C1, AC007450; RP11-438I19 (438I19), N0438I19.

PCR primers used to amplify breakpoints

PCR primers used to amplify junction sequences of the breakpoints in J20 were as follows: breakpoint (BP) 1, CTTATGTCTCACTTGGGCAC (108462-108443 in 150C16) and CCTTCACTTCACTTGTTAGC (113076-113057 in 425I22); BP2, TTCCTACAGAGCCAAAATGCCA (111355-111376 in 366L20) and ACTGCAACACCTCTCTAGCAG (109879-109899 in 425I22); BP3, TTGAACCCTTTGCCATTACGT (111047-111027 in 425I22) and TATTTAACACCTATCTGACTCC (97995-98016 in 150C16). Primers, GTGCCCAAGTGAGACATAAG (108443-108462 in 150C16) and TGTTGACTGAGCCCCATGAT (108598-108579 in 150C16), were used for positive control PCR.

Junction sequences of the breakpoints in US1 were confirmed by PCR with the following primer mixture to amplify both normal and abnormal alleles at the same time: BP5, CCAAAAGTGGGCTTACA-CATAAAA (44148-44125 in 474P2), TTCGCTCCTCCCACCTCATA (primer A, 111517-111498 in 366L20), and ACTCCCTGTAGTGAATC-CTCTGTTTAGA (primer B, 111043-111070 in 366L20); BP6, GC-CCGGGTTAATGTCGCTGAAT (37462-37483 in 474P2), GTT-GGGGGTGGGGACAAAATG (primer C, 30520-30540 in 434C1), and CGTTGGCAAAGCAGGGTTCCT (primer D, 31301-31281 in 434C1); BP7, GAAGCTCCAACTTTGCCCTCTG (88565-88586 in 221N13), primer B and primer A; and BP8, GGGCAGTTGGAATTGGGGAGAT (89202-89181 in 221N13), primer D and primer C.

Fluorescence in situ hybridization (FISH)

BAC clones 471G7, 150C16, and 366L20 were used as probes against hybrid cell lines derived from J20 and 438I19; 474P2 and 366L20 were used against bone marrow cells from US1. Signals were detected with biotinylated BAC probes and fluorescein isothiocyanate (FITC)-conjugated avidin (Vector Laboratories, Burlingame, CA) and amplified by using biotinylated antiavidin antibody (Vector Laboratories) and FITC-conjugated avidin. Chromosomes were stained with propidium iodide and mounted with glycerol-based medium containing 1,4-diazabicyclo(2,2,2)octane antifade. The chromosomal localization was captured through a PlanApochromat objective lens (63×/1.4 NA oil objective) using a Zeiss laser-scanning LSM510 microscope (Carl Zeiss, Jena, Germany) for J20 samples and through a Leica HCS PL FLUOTAR objective lens (100×/0.6-1.3 NA oil objective) using a Leica fluoromicroscope DM RXA2 with a Leica DC350F digital camera (Leica Microsystems, Wetzlar, Germany) for US1. Images were analyzed using Zeiss LSM510 software or Leica QFluoro software, respectively, and were processed with Adobe Photoshop (Adobe Systems, San Jose, CA).

Real-time PCR

Marrow samples were collected from J20 and US1, and control samples from healthy donors were purchased from a commercial vendor (Cambrex, Walkersville, MD). $CD59^-$ cells were isolated from the J20 sample by cell sorting (Becton Dickinson, San Jose, CA). Random hexamer-primed RNA from these samples was reverse transcribed using Superscript III (Invitrogen, Carlsbad, CA).

On the basis of the sequence of *HMGA2*, the following PCR primers and TaqMan MGB probe were designed: forward primer, 5′-TTC-AGCCCAGGGACAACCT (located in exon 1); reverse primer, 5′-TCTT-GTTTTTGCTGCCTTTGG (located in exon 2); TaqMan MGB probe, 6-carboxy-fluorescein (FAM)–AGCAAGAACCAACCGGT–non-fluorescent quencher–Minor groove binder (MGB) (the sequence of the probe spanned the boundary between exons 1 and 2) (Applied Biosystems, Foster City, CA). The method for amplifying β-glucuronidase cDNA as an internal control has been published.[13] PCR was performed using QuantiTect Multiplex PCR Kit (QIAGEN, Valencia, CA) on an ABI 7900HT sequence detection system according to the manufacturer's instructions (Applied Biosystems).

Measurement of allele frequency

Real-time PCR was used to measure the ratio of der(12) to normal chromosome 12 in hematopoietic cells of US1. Primers were designed around one of the breakpoints for detection of der(12). For detection of the wild-type allele, a region deleted in der(12) was analyzed. To measure the frequency of mutant *PIGA*, exon 2 was amplified, and PCR products were cloned into pGEM-Teasy vector (Promega, Madison, WI) and sequenced.

Analysis of allele-specific expression of *HMGA2*

The previously described polymorphic marker in the 5′ UTR of *HMGA2* was used to determine allele-specific gene expression in bone marrow cells[14] using the following primers: 5′-GACCCTATCCCGGCGGAGTCTC and 5′-TTGAAATGTTAGGCGGGGAAAGAA. DNA from hybridoma cell lines carrying one chromosome 12 was used to determine the origin of each allele. PCR fragments were separated by 15% to 25% gradient polyacrylamide gel electrophoresis (PAGmini; Daiichi Pure Chemicals, Tokyo, Japan).

Results

Patients

At age 33, J20 presented with pancytopenia and a hypocellular marrow without karyotypic abnormalities.[15] Five months later, an abnormal karyotype, 46, XX, t(12;12)(q13;q15), was reported in 3 (14%) of 21 metaphase cells. One year after diagnosis, blood counts were essentially normal, and marrow analysis showed normal cellularity with mild erythroid dysplasia. Cytogenetic analysis indicated expansion of the mutant clone with 10 (50%) of 20 metaphase cells having the abnormal karyotype. Laboratory evidence of hemolysis was noted, and flow cytometry showed 55% to 60% $GPI\text{-}AP^-$ erythrocytes. A mutation in exon 2 of *PIGA* (G715A) was shown in patient neutrophils.[15] Marrow mononuclear cells were separated into $GPI\text{-}AP^+$ and $GPI\text{-}AP^-$ populations, and the abnormal karyotype was found only in $GPI\text{-}AP^-$ cells.[15] These findings established the somatic nature of both the *PIGA* mutation and the chromosome 12 rearrangement and suggested that both genetic abnormalities were involved in the pathogenesis of clonal hematopoiesis.

US1 was 31 years old at presentation with complaints of fatigue and dark urine. Her white blood cell count was 4.1×10^9/L (4100/μL), hemoglobin level was 38 g/L (3.8 g/dL), and platelet count was 171×10^9/L (171 000/μL). Laboratory studies indicated intravascular hemolysis, and flow cytometry showed 88% $GPI\text{-}AP^-$ neutrophils. Marrow analysis revealed normal cellularity with erythroid hyperplasia without dysplasia and a karyotype of 46, XX, ins(12)(p12~13q13q12) in 20 (100%) of 20 metaphases. FISH showed the insertion split the *TEL* locus at 12p13. The abnormal karyotype was identified in 23% of mitogen-stimulated lymphocytes. A 14-bp deletion in the 3′ end of exon 2 of *PIGA* (693-706) was identified in neutrophil DNA. These findings confirmed the somatic nature of both the der(12) and mutant *PIGA* in US1.

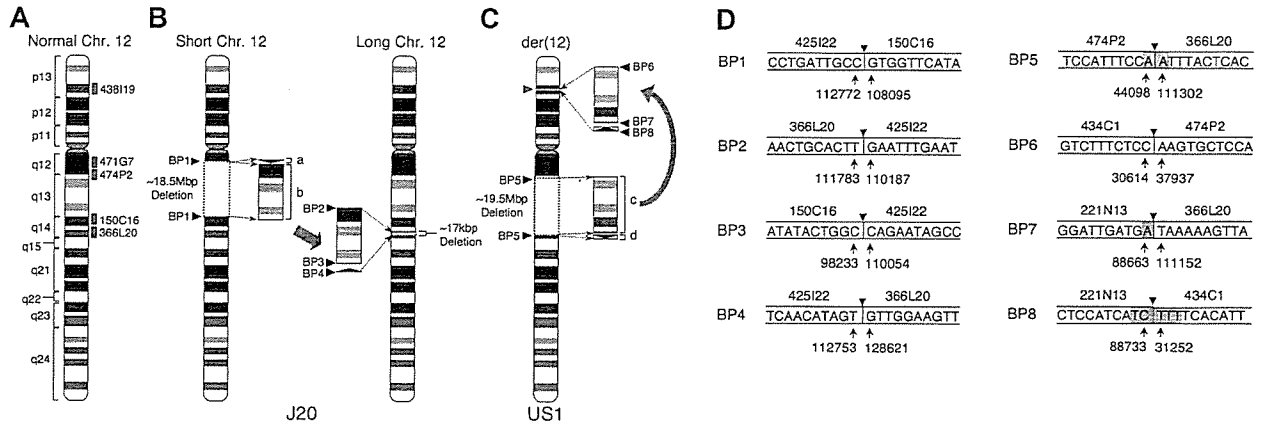

Figure 1. Chromosomal abnormalities in 2 patients with PNH. (A) Idiogram of normal chromosome 12 (Chr 12) modified from the NCBI Map viewer. Labeled gray boxes indicate the positions of the designated BAC clones used for FISH analysis. (B) J20. The karyotypic abnormality identified in the GPI-AP$^-$ bone marrow cells of J20 was defined as an interchromosomal insertion. An 18.5M-bp region from q12 to q14 (surrounded by broken lines) is deleted in short chromosome 12 as defined by characterization of BP1. The 2.7-kbp small fragment (bracketed arrowhead, labeled a) and the 18.5-Mbp large fragment (bracketed rectangle, labeled b) deleted from short chromosome 12 are inserted inversely and directly, respectively, into the 12q14 region of long chromosome 12 generating BP2, BP3, and BP4. The deleted region into which the 2 fragments are inserted lacks 17 kbp of sequence (broken lines). BP1, BP2, BP3, and BP4 indicate the breakpoint junctions generated by the chromosomal abnormality. (C) US1. The karyotypic abnormality identified in the bone marrow cells of US1 was defined as an intrachromosomal insertion. The large fragment (19.5 Mbp, labeled c) and the small fragment (300 kbp, labeled d) are inserted into the *TEL* locus (gray arrowhead) on 12p13. BP5 is generated by the deleted region. BP6, BP7, and BP8 are generated by rearranged fragments c and d. (D) Sequences of BP junctions in J20 and US1. The sequences around BP junctions 1 to 8 are shown. BAC clones containing the sequence are denoted above the lines. Arrows indicate the nucleotide numbers of the BAC clones. Arrowheads indicate one of the candidate breakpoints, and gray regions indicate ambiguous sequences shared between the 2 BAC clones at the site of the breakpoint.

Chromosomal abnormalities

Hybrid cell lines between patient monocytes and mouse myeloma cells were established. From J20, 2 lines (S1 and S2) carrying short chromosome 12 and 2 lines (L1 and L2) carrying long chromosome 12 (Figure 1B) were developed.[11] From US1, hybrid cells carrying normal chromosome 12 (US1W) or der(12) (US1M) were developed (Figure 1A,C). Chromosomal abnormalities (Figure 1) were delineated by using a combination of PCR analysis based on sequence-tagged site markers, FISH (Figure 2), Southern blotting, and inverse PCR (not shown).

For J20, the abnormality was defined as insertion of an 18.5-Mbp fragment derived from one chromosome 12 (short chromosome 12) into the other (long chromosome 12) (Figure 1B). The small fragment (a) and the large fragment (b) derived from the deleted region of short chromosome 12 were inversely and directly, respectively, inserted into 12q14 of long chromosome 12, generating BP2, BP3, and BP4 (Figure 1B).

For US1, the abnormality was an intrachromosomal insertion. The large fragment (19.5 Mbp, labeled c) and the small fragment (300 kbp, labeled d) derived from a region deleted from 12q13q14 are inserted inversely and directly, respectively, into the *TEL* locus on 12p13 (Figure 1C).

A combination of Southern blotting (not shown), PCR (Figure 2A-B), and FISH (Figure 2C-D) were used to confirm that breakpoints that defined the karyotypic abnormalities were present in peripheral blood and bone marrow of J20 and US1.

For J20, only GPI$^-$ cells had the chromosome 12 abnormality.[15] To investigate whether cells of US1 were also double mutants, the percentage of marrow cells with der(12) and mutant *PIGA* was quantitated. Mutant *PIGA* and der(12) were found in 91.8% and 93.9%, respectively, of bone marrow cells, indicating that the 2 mutations coexisted in the same cells. Together, these observations show that clonal hematopoiesis in these 2 patients is derived from a hematopoietic stem cell with somatic mutations of both *PIGA* and chromosome 12.

Effects of chromosome 12 abnormalities

Although the molecular details are different (Figure 1), the result of the chromosome 12 rearrangements is almost identical for the 2 patients, because in both cases, *HMGA2* is disrupted in the 3′ UTR of exon 5 (Figure 3A). No other effects of chromosome 12 rearrangement were detected for either J20 or US1. For US1, chimeric transcripts derived from *TEL* and *HMGA2* were not detected, and *TEL* transcripts appeared normal both quantitatively and qualitatively (not shown).

Real-time PCR showed that relative expression of *HMGA2* in bone marrow cells of both J20 and US1 was greater than normal (Figure 3B). In addition to rearranged *HMGA2*, both J20 and US1 have one intact *HMGA2* locus (Figure 1). To determine the allelic origin of *HMGA2* expression, a polymorphic region in the 5′ UTR[14] was analyzed. For both patients, *HMGA2* expression was derived almost exclusively from the rearranged locus (Figure 3C).

Discussion

These studies showed, in *PIGA*-mutant cells of 2 patients, rearrangement of chromosome 12 (Figures 1-2) that resulted in ectopic expression of *HMGA2* (Figure 3). The findings identify for the first time a molecular mechanism for clonal expansion of hematopoiesis in PNH.

HMGA2 is a member of the high-mobility group of proteins (HMGA1a, HMGA1b, HMGA2) that function as architectural transcription factors.[16-18] HMG members possess no intrinsic transcriptional activity. Instead, these nonhistone proteins orchestrate assembly of stereospecific transcriptional regulatory proteins into enhanceosomes.[18,19] The cellular targets of HMGA2 are incompletely defined but appear to include cyclin A.[19]

Molecular studies established a causal role for *HMGA2* in benign mesenchymal tumors.[17,20] Rearrangement of 12q13-15 is observed in these neoplasms, but tumorigenesis does not depend on generation of chimeric proteins derived from fusion of *HMGA2*

with specific translocation partners. Rather, clonal expansion induced by *HMGA2* appears to result from deregulated expression of a truncated version of the protein.[21-23] For the 2 patients with PNH, ectopic expression appears to be a consequence of gain-of-function mutational events (Figure 3B) caused by disruption of the 3′ UTR (Figure 3A) shown to contain elements that negatively regulate *HMGA2* transcription.[24] This hypothesis is supported by experiments showing that *HMGA2* transcripts from marrow of J20 and US1 are derived almost exclusively from the rearranged alleles (Figure 3C). Additional studies will be required to determine whether aberrant expression of *HMGA2* underlies clonal expansion in patients with PNH without structural abnormalities of 12q13-15.

PNH manifests many of the characteristics of a benign tumor because there is limited expansion of *PIGA* mutant clones (the peripheral blood of patients is a relatively stable mosaic of normal and abnormal cells), *PIGA*-mutant cells respect tissue boundaries

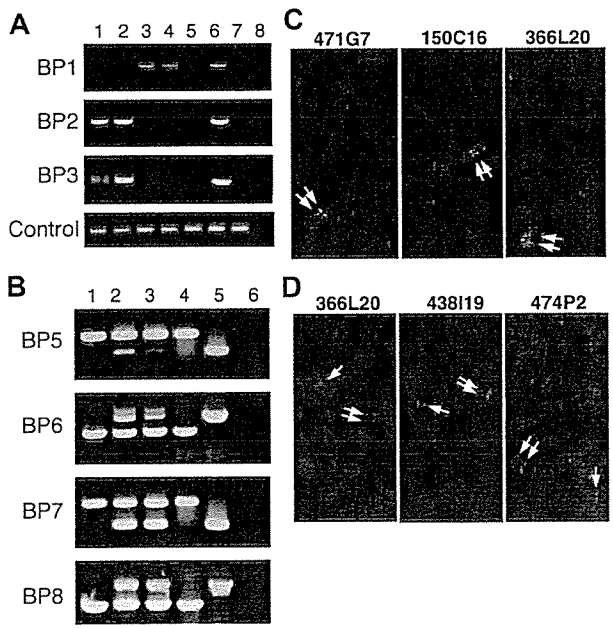

Figure 2. Confirmation of breakpoint junctions generated by the chromosomal abnormalities. (A) Confirmation of the breakpoints in J20 by PCR. Genomic DNA from L1 (lane 1), L2 (lane 2), S1 (lane 3), S2 (lane 4), JY25 (the wild-type control) (lane 5), white blood cells (WBCs) from J20 (lane 6), WBCs of a healthy volunteer (lane 7), or no DNA template (negative control, lane 8) was used for PCR analysis using primer sets designed according to the flanking regions of BP1, BP2, and BP3 (illustrated in Figure 1). Both the integrity and quantity of the DNA templates were confirmed by PCR using control primers (labeled Control). That appropriate-sized PCR products were amplified using DNA derived from the circulating WBCs of J20 (lane 6) shows that both the S1 and L1 versions of chromosome 12 were present in vivo. (B) Confirmation of the breakpoints in US1 by PCR. Genomic DNA from WBCs of a healthy volunteer (lane 1), bone marrow cells of US1 (lane 2), PMN of US1 (lane 3), US1W (the hybrid cell line containing wild-type chromosome 12) (lane 4), or US1M [the hybrid cell line containing (der(12)] (lane 5), or no DNA template (negative control, lane 6) were used for PCR analysis using primer sets designed according to the sequence of flanking regions of the BP5, BP6, BP7, and BP8 (illustrated in Figure 1). These experiments show that both wild-type chromosome 12 and der(12) were present in the peripheral blood and bone marrow of US1. (C) Metaphase FISH showing the chromosomal abnormality in J20. BAC probes 471G7, 150C16, and 366L20 were hybridized against chromosomal specimens derived from the cell line (L1) that contains only long chromosome 12. Two hybridization signals (arrows) were detected with all 3 BAC probes, confirming that long chromosome 12 contained the inserted material deleted from short chromosome 12. (D) Metaphase FISH showing the chromosomal abnormality in US1. BAC probes 366L20, 438I19, and 474P2 (illustrated in Figure 1) were hybridized with chromosomal specimens derived from bone marrow cells of US1. Each sample contained a der(12) (indicated by 2 hybridization signals on the same chromosome, double arrows) and a wild-type chromosome 12 (indicated by one hybridization signal, arrow). The intrachromosomal insertion splits the signal on 12p generated by hybridization of probe 438I19, whereas signals are generated on 12q and 12p when probes that overlap BP5 on the centromeric (474P2) and telomeric (366L20) ends are used.

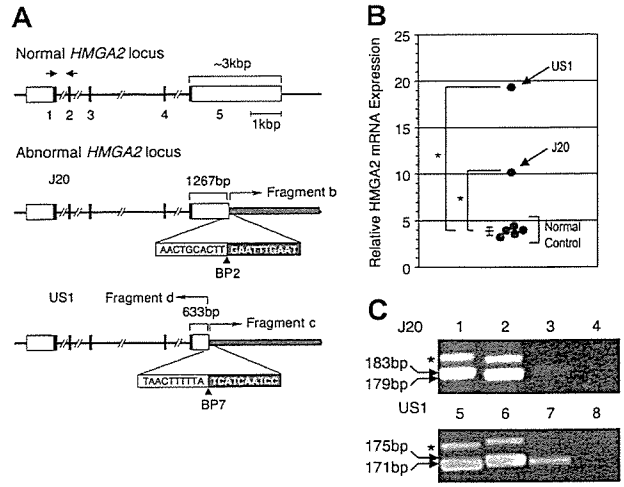

Figure 3. Effects of the chromosome 12 abnormalities in 2 patients with PNH. (A) Structure of normal and abnormal *HMGA2* locus in J20 and US1. White, black, and gray boxes indicate UTRs, coding regions, and abnormally fused fragments, respectively. The exon numbers of *HMGA2* are shown below the boxes. The nucleotide sequences on both sides of BP2 and BP7 (arrowheads) are shown in the white and gray boxes. The truncated *HMGA2* exon 5 of J20 and US1 are indicated by the brackets with the size (bp) shown above the brackets. The bent arrows indicate the fused fragments. The 3′ UTR of exon 5 of *HMGA2* on long chromosome 12 is disrupted as a result of insertion of fragment b (the 12q12q14 fragment from short chromosome 12; see Figure 1). In the case of US1, a similar disruption of exon 5 resulted from the rearrangement that occurred when material deleted from 12q (fragments c and d) was inserted into 12p (see Figure 1). (B) Real-time PCR analysis of HMGA2 transcripts in J20 and US1. The amount of *HMGA2* transcripts in bone marrow cells of 5 healthy individuals and of patients J20 and US1 were quantitated by using the TaqMan MGB PCR method. The positions of the forward (right-facing arrow) and reverse (left-facing arrow) PCR primers are indicated above the normal *HMGA2* locus shown in panel A. The relative expression of *HMGA2* transcripts is normalized to expression of β-glucuronidase transcripts. Each value of the relative expression indicates the average of triplicate measurements. Expression of HMGA2 was greater than normal (mean ± SD, 3.87 ± 0.45) for both J20 (mean, 10.23) and US1 (mean, 19.34) (*$P < .01$). The long and short horizontal bars indicate average and standard deviation (SD) in healthy individuals, respectively. (C) Allele-specific expression of HMGA2. A polymorphic region (based on TC repeats) in the 5′ UTR of *HMGA2* was amplified by PCR and analyzed by polyacrylamide gel electrophoresis. The products were also cloned and sequenced to characterize the polymorphisms. (Top panel) A 183-bp product (containing 29 TC repeats) was generated from the J20-derived hybrid cell line containing long chromosome 12 (lane 1), whereas a 179-bp product (containing 27 TC repeats) was generated from the cell line containing short chromosome 12 (lane 2). Analysis of the PCR product generated by amplification of cDNA derived from GPI-AP$^-$ bone marrow cells of J20 revealed only the 183-bp product (lane 3). No PCR products were visualized when the PCR template was prepared without reverse transcriptase (lane 4). (Bottom panel) A 171-bp product (containing 23 TC repeats) was generated from the US1 hybrid cell line containing the der(12) (lane 5), whereas a 175-bp product (containing 25 TC repeats) resulted from amplification of DNA from the cell line containing normal chromosome 12 (lane 6). Analysis of the PCR product generated by amplification of cDNA derived from unfractionated bone marrow cells of US1 revealed only the 171-bp product (lane 7). No PCR products were visualized when the PCR template was prepared without reverse transcriptase (lane 8). The asterisk (left of each panel) indicates the position of an uncharacterized PCR product. The abnormal allele-specific expression of HMGA2 in the bone marrow cells of US1 was confirmed by using a genetic analyzer (3100-Avant; Applied Biosystems) (not shown). For both J20 and US1, *HMGA2* expression appears to be derived exclusively from the mutant allele.

(there is no invasion of nonhematopoietic tissues), *PIGA*-mutant cells respond appropriately to signals that normally regulate hematopoiesis (function is not autonomous) and transformation into acute leukemia occurs rarely (PNH is not a premalignant condition).[25] Our studies suggest the concept of PNH as a benign tumor of the bone marrow with aberrant expression of *HMGA2* acting in concert with mutant *PIGA* (and the consequent deficiency of GPI-APs) to produce the proliferative phenotype that underlies clonal expansion. However, our studies neither establish the sequence of events that culminated in the clonal outgrowth of the

double mutant cells nor define how the aberrant expression of *HMGA2* works additively or synergistically with mutant *PIGA* to produce the proliferative phenotype. This latter issue will be the subject of future studies.

Findings reported herein provide new insights into the cause of the nonmalignant clonal hematopoiesis of PNH. Together with observations of others,[6,7] our studies support a 2-step process consisting of clonal immunoselection based on phenotype (ie, GPI-AP deficiency resulting from mutant *PIGA*) and clonal expansion as a consequence of a second somatic mutation that bestows the proliferative advantage. Clonal immunoselection may induce exit of *PIGA*-mutant stem cells from a dormant state,[4] thereby favoring acquisition of the mutation that underlies clonal expansion. But the benign nature of PNH suggests that genes involved in clonal expansion of *PIGA*-mutant stem cells are different from those that underlie malignant clonal diseases such as acute leukemia. Characterizing the molecular basis of benign clonal hematopoiesis is important not only for understanding the pathobiology of PNH but also for developing novel strategies for treatment of bone marrow failure and for enhancing stem cell function for both transplantation and gene therapy.

Acknowledgments

We thank Andrew Zinn (The University of Texas Southwestern Medical School at Dallas) and Kiran Chada (Robert Wood Johnson Medical School, University of Medicine and Dentistry of New Jersey) for helpful discussions, and Kiyo Kawata, Fumiko Ishii-Mori, and Keiko Kinoshita for technical assistance.

This work was supported by grants from the Ministry of Education, Culture, Sports, Science, and Technology of Japan; the Ministry of Health, Labour, and Welfare of Japan (T.K. and N.I.); the Osaka Medical Research Foundation for Incurable Diseases (N.I.); the Mochida Memorial Foundation for Medical Pharmaceutical Research (N.I.); the Japan Health Sciences Foundation (J.-I.N.); and the National Institutes of Health (grant K23 RR020043) (G.M. and C.J.P.).

Authorship

Contribution: N.I. designed research, performed research, and wrote the paper; T.I.-S. designed and performed research; Y.M., Y.E., and J.-I.N. performed research; K.K. contributed bioinformatics expertise; M.K., H.S., T.M., and Y.K. collected data; G.M. performed research; C.W. designed research; Z.C. performed research; W.B. and D.F.-L. provided essential material; and C.J.P. and T.K. designed research and wrote the paper.

Conflict-of-interest disclosure: The authors declare no competing financial interests.

N.I. and T.I.-S. contributed equally to this study.

Correspondence: Taroh Kinoshita, Department of Immunoregulation, Research Institute for Microbial Diseases, Osaka University, 3-1 Yamadaoka, Suita, Osaka 565-0871, Japan; e-mail: tkinoshi@biken.osaka-u.ac.jp.

References

1. Takeda J, Miyata T, Kawagoe K, et al. Deficiency of the GPI anchor caused by a somatic mutation of the PIG-A gene in paroxysmal nocturnal hemoglobinuria. Cell. 1993;73:703-711.
2. Miyata T, Takeda J, Iida Y, et al. The cloning of PIG-A, a component in the early step of GPI-anchor biosynthesis. Science. 1993;259:1318-1320.
3. Parker C, Omine M, Richards S, et al. Diagnosis and management of paroxysmal nocturnal hemoglobinuria. Blood. 2005;106:3699-3709.
4. Hu R, Mukhina GL, Piantadosi S, Barber JP, Jones RJ, Brodsky RA. PIG-A mutations in normal hematopoiesis. Blood. 2005;105:3848-3854.
5. Kawagoe K, Kitamura D, Okabe M, et al. Glycosylphosphatidylinositol-anchor-deficient mice: implications for clonal dominance of mutant cells in paroxysmal nocturnal hemoglobinuria. Blood. 1996;87:3600-3606.
6. Rotoli B, Luzzatto L. Paroxysmal nocturnal haemoglobinuria. Baillieres Clin Haematol. 1989;2:113-138.
7. Young NS, Maciejewski JP. Genetic and environmental effects in paroxysmal nocturnal hemoglobinuria: this little PIG-A goes "Why? Why? Why?" J Clin Invest. 2000;106:637-641.
8. Sugimori C, Chuhjo T, Feng X, et al. Minor population of $CD55^{-}CD59^{-}$ blood cells predicts response to immunosuppressive therapy and prognosis in patients with aplastic anemia. Blood. 2006;107:1308-1314.
9. Frickhofen N, Heimpel H, Kaltwasser JP, Schrezenmeier H. Antithymocyte globulin with or without cyclosporin A: 11-year follow-up of a randomized trial comparing treatments of aplastic anemia. Blood. 2003;101:1236-1242.
10. Inoue N, Murakami Y, Kinoshita T. Molecular genetics of paroxysmal nocturnal hemoglobinuria. Int J Hematol. 2003;77:107-112.
11. Inoue N, Izui T, Kuwayama M, et al. A possible intrinsic mechanism for clonal expansion of PNH abnormal cells. In: Omine T, Kinoshita T, eds. Paroxysmal Nocturnal Hemoglobinuria and Related Disorders. Tokyo, Japan: Springer-Verlag; 2003:117-126.
12. Hollander N, Selvaraj P, Springer TA. Biosynthesis and function of LFA-3 in human mutant cells deficient in phosphatidylinositol-anchored proteins. J Immunol. 1988;141:4283-4290.
13. Beillard E, Pallisgaard N, van der Velden VH, et al. Evaluation of candidate control genes for diagnosis and residual disease detection in leukemic patients using 'real-time' quantitative reverse-transcriptase polymerase chain reaction (RQ-PCR): a Europe against cancer program. Leukemia. 2003;17:2474-2486.
14. Ashar HR, Tkachenko A, Shah P, Chada K. HMGA2 is expressed in an allele-specific manner in human lipomas. Cancer Genet Cytogenet. 2003;143:160-168.
15. Nishimura JI, Inoue N, Azenishi Y, et al. Analysis of PIG-A gene in a patient who developed reciprocal translocation of chromosome 12 and paroxysmal nocturnal hemoglobinuria during follow-up of aplastic anemia. Am J Hematol. 1996;51:229-233.
16. Grosschedl R, Giese K, Pagel J. HMG domain proteins: architectural elements in the assembly of nucleoprotein structures. Trends Genet. 1994; 10:94-100.
17. Hess JL, Kossev P. Molecular genetics of benign tumors. Cancer Invest. 2002;20:362-372.
18. Reeves R. Molecular biology of HMGA proteins: hubs of nuclear function. Gene. 2001;277:63-81.
19. Tessari MA, Gostissa M, Altamura S, et al. Transcriptional activation of the cyclin A gene by the architectural transcription factor HMGA2. Mol Cell Biol. 2003;23:9104-9116.
20. Fedele M, Battista S, Manfioletti G, Croce CM, Giancotti V, Fusco A. Role of the high mobility group A proteins in human lipomas. Carcinogenesis. 2001;22:1583-1591.
21. Arlotta P, Tai AK, Manfioletti G, Clifford C, Jay G, Ono SJ. Transgenic mice expressing a truncated form of the high mobility group I-C protein develop adiposity and an abnormally high prevalence of lipomas. J Biol Chem. 2000;275:14394-14400.
22. Baldassarre G, Fedele M, Battista S, et al. Onset of natural killer cell lymphomas in transgenic mice carrying a truncated HMGI-C gene by the chronic stimulation of the IL-2 and IL-15 pathway. Proc Natl Acad Sci U S A. 2001;98: 7970-7975.
23. Battista S, Fidanza V, Fedele M, et al. The expression of a truncated HMGI-C gene induces gigantism associated with lipomatosis. Cancer Res. 1999;59:4793-4797.
24. Borrmann L, Wilkening S, Bullerdiek J. The expression of HMGA genes is regulated by their 3'UTR. Oncogene. 2001;20:4537-4541.
25. Hillmen P, Lewis SM, Bessler M, Luzzatto L, Dacie JV. Natural history of paroxysmal nocturnal hemoglobinuria. N Engl J Med. 1995;333:1253-1258.

The presence of anti-phosphatidylserine/prothrombin antibodies as risk factor for both arterial and venous thrombosis in patients with systemic lupus erythematosus

Junzo Nojima
Yoshinori Iwatani
Etsuji Suehisa
Hirohiko Kuratsune
Yuzuru Kanakura

In an effort to clarify the clinical significance of anti-phospholipid antibodies aPL detected by enzyme-linked immunosorbent assay ELISA, we examined the prevalence of anti-cardiolipin antibodies aCL, anti- β2-glycoprotein I antibodies (anti-β2-GPI), anti-prothrombin antibodies anti-PT, and anti-phosphatidylserine/prothrombin antibodies anti-PS/PT in 175 patients with systemic lupus erythematosus SLE comprising 67 patients with thrombotic complications. The present study showed that positive results of anti-β2-GPI-ELISA and anti-PS/PT-ELISA could serve as markers of thrombotic complications in patients with SLE, whereas aCL and anti-PT are less reliable as markers of these complications. Furthermore, results of the anti-PS/PT-ELISA correlate best with the occurrence of both arterial and venous thrombosis in patients with SLE.

Key words: anti-phospholipid antibodies, systemic lupus erythematosus, anti-β2-glycoprotein I antibodies, anti-phosphatidylserine/prothrombin antibodies,

Haematologica 2006; 91:699-702

From the Laboratory for Clinical Investigation, Osaka University Hospital, Suita, Osaka 565-0871, Japan (JN, ES); Division of Biomedical Informatics, Course of Health Science, Osaka University Graduate School of Medicine, Suita, Osaka, Japan YI; Department of Health Science, Faculty of Health Science for Welfare, Kansai University of Welfare Science, 3-11-1 Kashiwara, Osaka 582-0026, Japan HK; Department of Hematology and Oncology, Osaka University Graduate School of Medicine, Suita, Osaka, Japan YK.

Correspondence:
Junzo Nojima, Central Laboratory for Clinical Investigation, Osaka University Hospital, 2-15 Yamadaoka, Suita, Osaka 565-0871, Japan. E-mail: nojima@hp-lab.med.osaka-u.ac.jp

Anti-phospholipid antibodies aPL ar e a distinct group of autoantibodies that appear in a variety of autoimmune diseases, particularly systemic lupus erythematosus SLE. [1,2] They are associated with clinical events such as arterial and/or venous thrombosis, and obstetric complications.[3] The term *anti-phospholipid syndrome* APS has been used to describe a condition in which these clinical manifestations are linked to the persistence of aPL.[4-6] Detection of anti-cardiolipin antibodies aCL by enzyme-linked immunosorbent assay ELISA and detection of lupus anticoagulant LA activity by phospholipid-dependent coagulation assays have been standardized for the diagnosis of APS.

A number of clinical studies have established that aCL and LA activity are present in approximately 40% of patients with SLE and that the presence of these aPL constitutes a risk factor for arterial and/or venous thrombosis.[7-9] Moreover, recent reports indicated that the presence of LA activity is the strongest risk factor for thrombotic events in patients with SLE.[10,11] However, LA activity detected by a phospholipid-dependent coagulation assay is heterogeneous with respect to the specificities and functional capacities of the antibodies.[12] Therefore, the detection of LA activity requires a careful, sequential series of steps. Despite internationally accepted guidelines and many efforts to improve the standardization of LA assays, it is very difficult to standardize the laboratory diagnosis of LA.

Recent data suggested that some aPL-specific ELISA may help to confirm the presence of LA activity.[13] Therefore, we examined the prevalence of aCL, anti-β2-glycoprotein I antibodies (anti-β2-GPI), antiprothrombin antibodies anti-PT, and anti-phosphatidylserine/prothrombin antibodies anti-PS/PT in 175 patients with SLE (164 females, 11 males; aged 10-75 years; mean 40.11 years; 32 with arterial thrombosis, 35 with venous thrombosis, 14 with fetal loss, 14 with thrombocytopenia, and 80 with no thrombotic complications) to investigate the role of these aPL in thrombotic complications. The concentrations of aCL, anti-β2-GPI, anti-PT, and anti-PS/PT were measured by four different aPL-specific ELISA systems as reported previously.[14-16] We judged the concentrations of aCL, anti-β2-GPI, anti-PT, and anti-PS/PT in each absorbance level [milliabsorbance units (mAU)]. The absorbance of blank wells (i.e. coated only with TBS) was subtracted from the absorbance in the antigen-coated wells to account for non-specific binding. Monoclonal anti-human β2-GPI and anti-human prothrombin were used in each assay as a positive control, and selected control plasma samples were used as negative controls. We also studied the concentrations of aCL, anti-β2-GPI, anti-PT, and anti-PS/PT in 80 healthy control subjects (staff members of Osaka University Hospital; 74 women, 6 men; aged 22-60 years old; mean, 39.8 years). The concentrations of these antibodies in the 80 healthy controls subjects were log-transformed to approximate Gaussian